Chem. Rev. 1992, 92, 1769–1797

Molecular Electric Moments from X-ray Diffraction Data

M. A. Spackman

Department of Chemistry, University of New England, Armidale, N.S.W. 2351, Australia

Received March 10, 1992 (Revised Manuscript Received September 14, 1992)

Contents

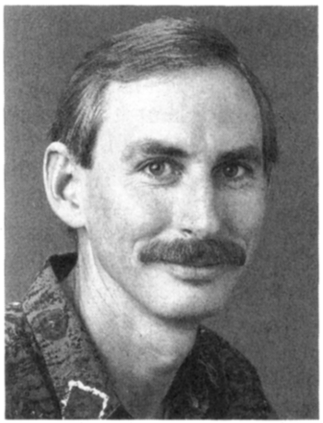

Mark A. Spackman was born in Australia in 1954 and received his B.Sc. degree in Chemical Physics (1976) and Ph.D. (1980) from the University of Western Australia. He arrived at the University of New England in 1987, after completing postdoctoral studies with R. F. Stewart (Carnegie-Mellon, 1980–1983), E. N. Maslen (Western Australia, 1983–1985) and B. M. Craven (Pittsburgh, 1985–1986). Currently a Senior Lecturer in the Department of Chemistry at UNE, his present research interests bridge the nexus between theoretical and experimental determinations of molecular properties.

I. Introduction

Electric multipole moments of molecules are useful. On a very fundamental level they are compact summaries of the molecular charge distribution (i.e., the distribution of *both* positive and negative charge) and as such provide insight into the nuclear and electronic structure of molecules. Increasingly, however, electric multipole moments of molecules are finding use in the study of intermolecular interactions. Numerous excellent review articles and books discuss applications and uses of multipole moments, especially to the interactions between molecules, and the reader is referred to those sources.[1–10]

It has long been known that electron distributions determined from X-ray diffraction data are a potential source of reliable electric moments of molecules. In a 1970 review of molecular electric moments,[11] Buckingham noted such a capability, but observed that such methods were not then capable of high accuracy. Curiously, in the same year, Stewart[12] reported a dipole moment for uracil derived from point charges obtained from a valence monopole electron density model fitted to X-ray data. The value obtained by Stewart, 4.0 ± 1.3 D, predated by four years a capacitance measurement made in dioxane, which yielded $\mu = 4.16 \pm 0.4$ D,[13] yet only recently[14] has the X-ray value been regarded as a valid experimental measurement of the dipole moment of uracil, despite yielding not only μ but all three components of the dipole moment vector. Clearly Stewart's measurement of μ for uracil was accurate, although not as precise as we would like.

Unfortunately, in spite of a large number of determinations of molecular dipole moments, and a few molecular quadrupole moments, from X-ray diffraction data since 1970, it is not yet widely accepted that such determinations are valid experimental *measurements* of these quantities. It is the central thesis of this review article that such acceptance is now warranted, and that measurements of dipole, quadrupole, and higher moments of molecules from X-ray diffraction data can be competitive with other experimental techniques; in some cases results are obtained which are otherwise unattainable experimentally.

This article is aimed at those involved in the determination of electron distributions from diffraction data, those who determine electric moments using alternative experimental techniques, and also a more general audience. Driven by a need to emphasize the quality and the limitations of the results obtained to

0009-2665/92/0792-1769$10.00/0

date, we will be almost exhaustive in our presentation of results, briefly discussing each example in turn in section V. In section II we carefully define the lower electric moments in terms of first, second, and higher moments of the total charge distribution, and briefly discuss origin dependence and, most importantly, units. Section III contains a short description of other experiments which yield molecular electric moments, with particular emphasis on their respective strengths and limitations. The ensuing section outlines the various strategies currently employed for obtaining electric moments from X-ray diffraction data. In section V comparison of X-ray diffraction results is made with other experimental results and with ab initio theoretical calculations where appropriate.

It is strongly hoped that this review article will encourage more practitioners in the electron density field to analyze their X-ray data in this fashion and actually report electric moments. Furthermore, we hope to provide some incentive for more work on the critical evaluation of these important molecular properties determined from X-ray diffraction experiments.

II. Definition of Electric Moments

The literature on molecular electric multipole moments yields several different conventions for defining these properties. Generally, these differences arise from the context and use of the moments in a particular application, and the differences can usually be characterized as the *unabridged* convention[3,15,16] or the *traceless* convention.[1,2,11,17-19] The relationship between the unabridged and traceless moments is given in several of these works, and in a particularly clear fashion by Applequist[15] and McLean and Yoshimine[18] (but note that there is a difference of a factor of $n!$ in the definitions of the nth rank tensor in those two works). A slightly different convention defines the multipole moments in terms of the regular spherical harmonics.[20-22] This convention has been utilized in the recent studies of intermolecular interactions by Stone and co-workers.[8,23-27]

For the purposes of the present discussion we consider a molecular charge distribution in three dimensions, $\rho(\mathbf{r})$, consisting of a continuous electron density distribution (negatively charged) and a number of (positive) point charges arising from the nuclei. The *charge* of a molecule is the zeroth moment

$$q = \mu^{(0)} = \int_v \rho(\mathbf{r})\,\mathrm{d}\mathbf{r} \qquad (1)$$

where the integral is over the volume v containing the molecular charge distribution. The molecular charge is seldom of interest in electron density studies since it is usually zero; exceptions include studies of molecular ions (e.g. SO_4^{2-}, NH_4^+, and CN^- [28-30]), charge transfer complexes (e.g. TTF–TCNQ[31]), or the transfer of charge to water molecules in molecular crystals (e.g. oxalic acid dihydrate[32,33] or $NaCN{\cdot}2H_2O$[30]). Techniques for obtaining net molecular (or ionic) charges from X-ray diffraction data are identical to those used to derive higher moments (section IV).

A. First and Second Moments

In this work we define the first, second, and higher unabridged molecular moments in the manner of McLean and Yoshimine,[18] Hirshfeld,[34] and Moss.[35] Thus the components of the nth rank unabridged molecular electric multipole moment are given by

$$\mu^{(n)}_{\alpha\beta\ldots\eta} = \int_v \rho(\mathbf{r}) r_\alpha r_\beta \ldots r_\eta\,\mathrm{d}\mathbf{r} \qquad (2)$$

where Greek suffixes indicate the Cartesian indices x, y, or z. More specifically, the first moments are given by

$$\mu^{(1)}_x = \int_v \rho(\mathbf{r}) x\,\mathrm{d}\mathbf{r} \qquad (3)$$

for example and the second moments by

$$\mu^{(2)}_{xy} = \int_v \rho(\mathbf{r}) xy\,\mathrm{d}\mathbf{r} \quad \text{etc.} \qquad (4)$$

These definitions are simple and straightforward, and differ from those of Applequist by a factor of $n!$ for the nth moment.

B. Dipole and Quadrupole Moments

The components of the dipole moment are identical to those of the first molecular moment:

$$\mu_\alpha = \mu^{(1)}_\alpha = M^{(1)}_\alpha \qquad (5)$$

where the general nth rank traceless tensor component is given by

$$M^{(n)}_{\alpha\beta\ldots\eta} = \frac{(-1)^n}{n!}\int_v \rho(\mathbf{r}) r^{2n+1} \frac{\partial^m}{\partial r_\alpha \partial r_\beta \ldots \partial r_\eta}\left(\frac{1}{r}\right)\mathrm{d}\mathbf{r} \qquad (6)$$

Thus the components of the quadrupole moment tensor are

$$\Theta_{\alpha\beta} = \mathrm{M}^{(2)}_{\alpha\beta} = {}^1/_2 \int_v \rho(\mathbf{r})[3r_\alpha r_\beta - r^2\delta_{\alpha\beta}]\,\mathrm{d}\mathbf{r} \qquad (7)$$

Explicit expressions for components of octopole and hexadecapole moments are given elsewhere.[11,17,18] The components of the traceless quadrupole moment tensor can be readily derived from the second moments

$$\Theta_{xx} = \mu^{(2)}_{xx} - {}^1/_2(\mu^{(2)}_{yy} + \mu^{(2)}_{zz})$$

$$\Theta_{xy} = {}^3/_2 \mu^{(2)}_{xy} \qquad (8)$$

where the remaining components can be generated by permutation of x, y, and z. This relationship between the second moments and quadrupole moments is important for our discussion in section V. More general expressions involving higher moments are given by Applequist.[15]

For simplicity of notation we will drop the superscript (n) on $\mu^{(n)}$ and $M^{(n)}$ in the rest of this article. The first and second moments are then denoted simply by μ_α and $\mu_{\alpha\beta}$. It is also worthwhile commenting upon the various symbols used for the quadrupole and higher moments. Buckingham[11] uses ξ instead of M for the general case, and μ, Θ, Ω, Φ for dipole, quadrupole, octopole, and hexadecapole moments respectively; we adopt that convention for the individual moments, as it is now clearly accepted in the field. McLean and Yoshimine[18] denote the lower unabridged moments by μ, Q, R, and S, Böttcher et al.[16] use M, Q, and U for both unabridged and traceless dipole, quadrupole, and octopole moments. Hirschfelder et al.[9] also use Q for the traceless quadrupole moment, but its elements are defined to be twice those adopted elsewhere. More recently, Gray and Gubbins[3] use μ, Θ, and O for unabridged dipole, quadrupole, and octopole moment tensors, and Q for the traceless quadrupole moment. Clearly some care is needed in reading the literature and comparing results from different sources.

C. Origin Dependence

The definitions given in the previous two sections refer to a specific coordinate origin, which is arbitrary, but usually chosen within the charge distribution; it has become conventional to choose the center of mass, but for various reasons an alternative origin may be chosen, or dictated. Transformation of the components of unabridged and traceless tensors are given elsewhere in detail,[1,15,18] and we summarize here the results for the lower moments. For a translation of the axis system given by

$$r'_\alpha = r_\alpha - R_\alpha \qquad (9)$$

where $R_\alpha = (X, Y, Z)$ are the coordinates of the new coordinate origin in the original axis system

$$q' = q$$

$$\mu'_x = \mu_x - qX \text{ etc.,}$$

$$\mu'_{xx} = \mu_{xx} - 2\mu_x X + qX^2 \text{ etc.,}$$

$$\mu'_{xy} = \mu_{xy} - \mu_x Y - \mu_y X + qXY \text{ etc.,}$$

$$\Theta'_{xx} = \Theta_{xx} - 2\mu_x X + \mu_y Y + \mu_z Z + q[X^2 - {}^1/_2(Y^2 + Z^2)] \text{ etc.,}$$

and

$$\Theta'_{xy} = \Theta_{xy} - {}^3/_2(\mu_y X + \mu_x Y) + {}^3/_2 qXY \text{ etc.} \qquad (10)$$

Results for components not given explicitly can be obtained by permuting x, y, and z.

From these expressions it is easily seen that only the first, nonvanishing, moment is independent of origin. Thus if $q = 0$, as it will be for almost all examples we consider later, μ is independent of the choice of origin. However, Θ will only be origin independent provided that both q and μ are zero; i.e. for neutral nondipolar molecules. In our discussion of results in section V, all quadrupole moments are reported with respect to the molecular center of mass.

Molecular symmetry clearly determines whether μ will be zero or Θ independent of origin, but it also dictates the number of unique components of μ, Θ, Ω, etc. The number of constants required to completely specify these tensors has been tabulated by Buckingham.[1,7] For clarity, and because these results will be assumed in section V, specific examples are given here. For molecules with C_1 symmetry, three components of μ are required, six components of the second moment, and only five constants are needed to define Θ. If the molecule is axially symmetric (i.e. contains a 3-fold or higher rotation axis) there is just one unique component of any order molecular moment, and

$$\mu = \mu_\parallel$$

$$\Theta = \Theta_\parallel = -2\Theta_\perp \qquad (11)$$

where the subscripts $\parallel$ and $\perp$ denote components parallel to and at right angles to the symmetry axis, respectively.

D. Units

In addition to confusion with symbols, the literature on electric moments employs a variety of systems of units. In this work we use SI units where possible, but conversions to other systems such as atomic units (au), electrostatic units (esu), and special units such as Debye and Buckingham based upon the esu, are often necessary. X-ray diffraction results are often presented in units of electron Å (e Å) or electron Å^2 (e Å^2), compatible with the crystallographic unit of electron density, e Å^{-3}. Table I summarizes the conversion from one system to another for the lowest electric moments.

III. Other Sources of Electric Moments

A. Experimental Determination

There are now a multitude of experimental techniques which yield measurements or estimates of the lower electric moments, particularly the dipole moment, for which McClellan[14] lists nearly 100 different methods of determination or estimation. In this section we wish to furnish a background and provide a broader perspective to our discussion in section V; hence, we mention only the most common techniques for determining dipole and quadrupole moments, with particular emphasis upon the relative advantages, limitations, scope of applications, and accuracy and precision of the results.

1. Dipole Moments

Very broadly speaking, molecular dipole moments reported in the literature come from two types of experiments: one is the measurement of dielectric permittivity of gases, solutions or pure liquids; the other is from the Stark effect. There are several important tabulations of experimental dipole moments available. The most extensive is the three-volume compilation by McClellan[14,37,38] which provides a comprehensive summary of the literature to the end of 1981. Other tabulations include several volumes of the Landolt-Börnstein series[39] and review articles by Lovas and Tiemann.[40,41] The book by Huber and Herzberg[42] is an excellent reference for diatomic molecules.

a. Dielectric Permittivity. The Debye equation expresses the relationship between the relative dielectric permittivity, ϵ_r, and the molecular properties α (polarizability) and μ (dipole moment):

$$\frac{\epsilon_r - 1}{\epsilon_r + 2} = \frac{N_\mathrm{A}}{3V_\mathrm{m}\epsilon_0}(\alpha + \mu^2/3kT) \qquad (12)$$

This is usually expressed in terms of the molar polarization, $P_\mathrm{m} = V_\mathrm{m}(\epsilon_r - 1)/(\epsilon_r + 2)$:

$$P_\mathrm{m} = \frac{N_\mathrm{A}}{3\epsilon_0}(\alpha + \mu^2/3kT) \qquad (13)$$

and hence it would seem possible to determine α and

Table I. Dipole and Quadrupole (or Second) Moment Conversion Factors[a]

dipole moments

	e a_0	e Å	C m	esu	D
1 e a_0	1.0	0.529 177	$8.478\,36 \times 10^{-30}$	$2.541\,75 \times 10^{-18}$	2.541 75
1 e Å	1.889 73	1.0	$1.602\,18 \times 10^{-29}$	$4.803\,21 \times 10^{-18}$	4.803 21
1 C m	$1.179\,47 \times 10^{29}$	$6.241\,51 \times 10^{28}$	1.0	$2.997\,92 \times 10^{11}$	$2.997\,92 \times 10^{29}$
1 esu	$3.934\,30 \times 10^{17}$	$2.081\,94 \times 10^{17}$	$3.335\,64 \times 10^{-12}$	1.0	1.0×10^{18}
1 D	0.393 430	0.208 194	$3.335\,64 \times 10^{-30}$	1.0×10^{-18}	1.0

quadrupole and second moments

	e a_0^2	e Å^2	C m^2	esu	B
1 e a_0^2	1.0	0.280 029	$4.486\,55 \times 10^{-40}$	$1.345\,04 \times 10^{-26}$	1.345 04
1 e Å^2	3.571 06	1.0	$1.602\,18 \times 10^{-39}$	$4.803\,21 \times 10^{-26}$	4.803 21
1 C m^2	$2.228\,88 \times 10^{39}$	$6.241\,51 \times 10^{38}$	1.0	$2.997\,92 \times 10^{13}$	$2.997\,92 \times 10^{39}$
1 esu	$7.434\,75 \times 10^{25}$	$2.081\,94 \times 10^{25}$	$3.335\,64 \times 10^{-14}$	1.0	1.0×10^{26}
1 B	0.743 475	0.208 194	$3.335\,64 \times 10^{-40}$	1.0×10^{-26}	1.0

[a] Note that all entries on the same line are equal; the unit at the top of the column applies to all values below it. Fundamental constants are from Cohen and Taylor[36] (e = $1.602\,177\,33 \times 10^{-19}$ C, $a_0 = 0.529\,177\,249 \times 10^{-10}$ m, $4\pi\epsilon_0 = 10^7 c^{-2}$, $c = 2.997\,924\,58 \times 10^8$ m s^{-1}, esu of charge = $3.335\,640\,95 \times 10^{-10}$ C).

μ for a sample of molecules by measuring ϵ_r at a series of temperatures, calculating P_m and plotting it against T^{-1}. This in fact is the origin of most early accurate dipole moments for gaseous molecules.[43,44] P_m is related to the first dielectric virial coefficient, and as such requires low densities (or extrapolation to low densities) for accurate results, which can be obtained especially for strongly polar molecules. Measurements at higher gas densities yield valuable information on higher dielectric virial coefficients, and hence intermolecular interactions.

As most large organic molecules have a low vapor pressure, the vast majority of dipole moment measurements reported in the literature have been obtained by application of the Debye equation to dilute solutions in nondipolar solvents such as benzene, dioxane, or cyclohexane. Although strictly valid only for gases at low pressures, the Debye equation is a satisfactory approximation for dilute solutions under certain conditions.[45,46] The interaction between solute and solvent, referred to as the solvent effect, may change the apparent dipole moment from that which would be measured in the gas phase. Most importantly, the solvent effect is temperature-dependent and hence leads to serious errors in attempts to obtain μ as described above for gases.

Two alternative strategies have been adopted for measurement of dipole moments in solution: one is the calculation of P_m for solutions of different concentrations, followed by extrapolation to infinite dilution. The other is the direct extrapolation of the dielectric constant and the density as functions of solute weight fraction. Both strategies lead to similar results and suffer from the same overall drawback:[46] The solute polarization at infinite dilution is in error because of the solvent effect, which in turn is a function of molecular shape, dipole moment, and polarizabilities of solute and solvent, and may be negligibly small or may affect the dipole moment by as much as 10%, commonly lowering it. No matter how precise the measurements of ϵ_r, weight fraction, or refractive index, the absolute value of a dipole moment obtained from dilute solution measurements may be in error by as much as 10%, but usually by somewhat less. Smyth[46] discusses several empirical relationships which have found success in calculating an approximate "gas-phase" dipole moment from a value determined in dilute solution, given the relative permittivity of the solvent. No matter how reliable these empirical corrections may be, they can still only yield the magnitude of the dipole moment; dielectric measurements cannot yield information about the magnitude of all three components of μ, except in a limited number of special cases, usually for high-symmetry molecules.

A further characteristic of dipole moments obtained by dielectric permittivity measurement results from the statistical thermodynamic average involved in the derivation of (12) and is relevant in any comparison with X-ray diffraction results: μ is an effective dipole, assumed to be the same for all populated electronic, vibrational, and rotational states. In a sense it is a thermal average.

b. Stark Effect. Buckingham[47] gives a detailed description of the significance and application of the Stark effect in spectroscopy. Here we are concerned solely with its application to the determination of dipole moments of gases, where small changes in the rotational spectrum of a molecule, usually in the microwave region, are measured as functions of an applied electric field. The best of these measurements usually come from molecular beams[48] where μ can often be obtained accurate to 0.01%.

The most common gas-phase dipole-moment determinations derive from application of the Stark effect to microwave spectroscopy. Under favorable conditions it is possible to measure μ as a function of vibrational or rotational state. Because of this the measurement obtained refers to a specific quantum mechanical state, and not to a vibrational or thermal average. It is thus quite different from μ resulting from permittivity measurements. An excellent summary of the technique is given by Gordy and Cook,[49] who also list many examples of dipole moment determinations for diatomics, symmetric-top molecules, and asymmetric rotors. Typical precisions achieved vary from 1 or 2%, to better than 0.1% in favorable cases. However, for the present purpose it is noteworthy that only the absolute magnitudes of the dipole components along the three inertial axes can be determined from the rotational Stark effect. The direction of these components can often be assigned by use of other chemical information such as electronegativities or bond moments, but where a unique assignment is impossible, isotopic substitution is often a feasible alternative. The Zeeman effect (see below) can also yield the dipole moment direction.

2. Quadrupole Moments

Methods for the determination of molecular quadrupole moments have been summarized and described in detail elsewhere.[3,11,45] Most literature values have been obtained by direct measurements of the induced birefringence brought about by an electric field gradient or by the Zeeman effect in microwave spectroscopy or molecular beam experiments. A variety of indirect methods have also been employed, which have in common their dependence on an assumed intermolecular potential. Important tabulations of quadrupole moments include those by Stogryn and Stogryn,[17] Buckingham,[11] Flygare and co-workers[50,51] and more recently Appendix D in Gray and Gubbins' book.[3]

a. Induced Birefringence. The birefringence, Δn, induced in a gas by an electric field gradient is a function of the product of the polarizability tensor, α, and the traceless quadrupole moment tensor, Θ:[2,52]

$$\Delta n \propto \alpha_{\alpha\beta}\Theta^*_{\alpha\beta}/kT \tag{14}$$

where $\Theta^*_{\alpha\beta}$ is the molecular quadrupole moment with respect to the "effective quadrupole center". As for the Debye equation, a statistical thermodynamic average has been used to obtain this expression, and therefore the quadrupole moments derived via eq 14 relate to a thermal average, and not a specific quantum state. For molecules with a three-fold or higher rotation axis, the product in eq 14 reduces to $\Delta\alpha\Theta^*$, where $\Delta\alpha$ is the polarizability anisotropy and Θ^* the unique component of the quadrupole moment. Further, for centrosymmetric molecules the effective quadrupole center is the molecular center of symmetry, coincident with the center of mass, and hence $\Theta^* = \Theta_{zz}$.

From this discussion, it is clear that the electric field gradient induced birefringence technique is largely restricted to highly symmetric molecules which possess a center of symmetry, and in fact the great majority of applications have been to such molecules. The reader is referred to the recent work by Graham, Pierrus, and Raab[53] and Buckingham, Graham, and Williams[54] and references therein for details of measurements in the gas phase. Ritchie and co-workers[55-57] have extended the induced birefringence experiment to the study of larger molecules in dilute solutions, where eq 14 applies with appropriate modification. The current status of such experiments is described by Dennis and Ritchie,[57] who cite applications to systems as large as tri- and hexasubstituted benzenes, ferrocene, and ruthenocene.

The precision obtainable with these experiments is presently (0.2–0.5) × 10^{-40} C m^2 for gases,[53] and approximately (1.0–3.0) × 10^{-40} C m^2 in dilute solution;[57] many earlier measurements are considerably less precise. Limitations of the induced birefringence method include the general need for molecules of high symmetry, and for which the polarizability tensor is known reliably, the origin dependence of Θ^* for dipolar molecules, and the problems associated with choice of solvent and its effect on values obtained in dilute solution. Nevertheless, for nondipolar molecules, this is the most general method for direct measurement of Θ, and it is worth emphasizing that both induced birefringence and molecular Zeeman effect methods yield the sign *and* magnitude of Θ.

b. Zeeman Effect. The effect of a magnetic field (Zeeman effect) on the rotational spectra of polar molecules yields the magnetizability tensor, χ, and the dimensionless gyromagnetic tensor, g. Coupled with the moment of inertia tensor, I, these quantities yield the diagonal components of the second moment tensor relative to the inertial axes. The details of the theory have been discussed in detail by Gordy and Cook,[49] and Flygare and co-workers,[50,51,58,59] and those publications review most of the literature on the method. The second moments of course yield the diagonal components of the quadrupole moment, and results have been obtained for a large number of polar molecules. Like other experimental methods described above, the molecular Zeeman effect method for the determination of Θ offers several advantages and suffers from several limitations. Unlike the induced birefringence method, quadrupole moments are obtained with respect to the molecular center of mass and are defined with respect to the inertial axes. For molecules with high symmetry, the principal axes of I and Θ coincide, but for general unsymmetrical molecules (such as formic acid or formamide for example) both Θ and I generally possess off-diagonal components, but only the diagonal elements *in the inertial axis system* are generally determined. Recent work by Sutter and co-workers[60] has enabled the determination of the complete quadrupole moment tensor by a study of Zeeman rotational spectra for HNO_3 and DNO_3.

The derivation of Θ in terms of the observable tensors g, I, and χ typically involves the difference between two terms of comparable magnitudes; hence the relative error in components of Θ can often be quite large, despite a high relative precision in measurements of g or χ. The case of pyridine is typical, where the relative precision in g is 1% or better, that in χ is 1% to 2%, yet Θ has relative errors between 10% and 25%. For small components of Θ relative errors exceeding 100% are to be expected and are indeed obtained. Perhaps a better estimate of the precision of molecular Zeeman experiments is to examine absolute errors; values between 1.0 and 10.0 × 10^{-40} C m^2 are common. Higher precision is obtained in molecular beam applications of the molecular Zeeman effect, such as molecular beam electric (or magnetic) resonance and beam maser experiments. Dymanus[61] and Dyke and Muenter[62] give recent reviews of beam experiments. A typical result, relevant to the discussion in section V, is that obtained for water,[63] for which error estimates are as small as (0.07–0.10) × 10^{-40} C m^2 for all three components of Θ. Unfortunately, only a very small number of measurements of Θ have been reported from molecular beam experiments.

A limitation of the molecular Zeeman effect determination of Θ is its restriction to dipolar molecules. However, this is turned to advantage in the use of the origin dependence of Θ for dipolar molecules to determine the sign of μ. This is especially useful where μ is small, for example CO, where the molecular Zeeman effect was used to demonstrate the $^-CO^+$ polarity.[64]

c. Indirect Methods. The vast majority of molecules have not been studied by the above methods. For some, estimates of Θ have been obtained by so-called "indirect" methods, methods which infer a value of Θ (and often higher electric moments) by fitting intermolecular potential functions to experimental data which contains information on molecule–molecule interactions. These methods yield only the magnitude (or a bound), but not the sign of Θ. Data used for such purposes include pressure and dielectric second virial coefficients, heats of sublimation and other crystal properties, and pressure broadening in the microwave region. Buckingham[11] and Appendix D of Gray and Gubbins' book[3] list additional methods.

B. Ab Initio Methods

The ready availability of high-speed computational resources and the widespread use of ab initio quantum chemical packages such as GAUSSIAN,[65] GAMESS,[66] and CADPAC[67] have made the computation of molecular electric moments, especially the lower moments, by ab initio theoretical methods a viable alternative to experiment in many instances. There are, however, several complications which must be adequately dealt with in order to obtain *reliable* estimates (i.e. competitive with the best experimental determinations) for even the lower moments. These can be broadly categorized as basis set effects, electron correlation effects, and the problem of vibrational and rotational averages. The literature on the ab initio determination of molecular properties is considerable; we discuss here only those aspects relevant to our major theme.

Choice of basis set has been reviewed in detail by Davidson and Feller,[68,69] but the optimum selection for the computation of molecular moments was not emphasized. Dykstra and co-workers[70–72] discuss the rationale behind basis set selection and review in details many aspects of the determination of molecular properties using ab initio methods. A summary of dipole moment results using standard basis sets of the Pople group has been given by Hehre et al.[73] The consensus is quite clear: basis sets of at least double-ζ quality are required, with one, or preferably two, sets of polarization functions in order to reliably approach the Hartree–Fock limit.

The effect of electron correlation upon the lower electric moments has received increasing attention in recent years, and systematic studies with both configuration interaction (CI) and many-body perturbation theory (MBPT) approaches to the problem have been published.[74–77] The role of rotational and vibrational averaging of electric moments has been discussed by several authors recently,[70–72] usually with reference to diatomic molecules. Bishop[78] has recently discussed this topic in considerable depth.

In the present work we have computed ab initio dipole and quadrupole moments for comparison with diffraction results, particularly where no other measurements have been reported, because we feel it is important to establish the reliability (or otherwise) of the X-ray diffraction result. For this purpose we have chosen the widely used 6-31G** basis set[73,79–82] and perform calculations only at the self-consistent field (SCF) level. Although not an optimum choice of basis set or method for definitive calculations, this represents a compromise between accuracy of results and applicability to a majority of the large molecular systems for which X-ray diffraction results are available. The SCF/6-31G** model generally overestimates the experimental dipole moment, a fact that has been attributed to the tendency of the closely related 6-31G* basis to overemphasize the contribution of zwitterionic valence structures.[73] Because we are unaware of a similar assessment of SCF/6-31G** quadrupole moments, in Table II we compare those predictions for several small molecules with near Hartree–Fock and CI benchmark results obtained by Feller et al.[77] and with experiment. All ab initio calculations performed for the present work employed CADPAC on the Gould NP1 in the Computer Centre of the University of New England.

Table II. SCF/6-31G Dipole and Quadrupole Moments Compared with Near Hartree–Fock Limit SCF and Multireference Singles and Doubles CI (MRSD-CI) Results from Feller and Davidson,[77] and with Experiment Where Available[a]**

		6-31G** SCF	benchmark SCF	MRSD-CI	experiment
N_2	Θ_{zz}	−4.57	−4.17	−4.89	−4.72(26)[b]
CO	μ_z	−1.11	−0.89	0.34	0.4076(3)[c]
	Θ_{zz}	−7.23	−6.89	−6.83	−6.3[d]
HF	μ_z	−6.58	−6.42	−6.10	−6.0915(12)[e]
	Θ_{zz}	7.41	7.78	7.62	7.87(10)[f]
HCl	μ_z	−4.93	−4.04	−3.88	3.6976(17)[g]
	Θ_{zz}	12.38	12.60	12.27	12.48(40)[f]
NH_3	μ_z	−6.31	−5.39	−5.20	−4.908(5)[h]
	Θ_{zz}	−8.57	−9.69	−9.79	−7.74(23)[i]
PH_3	μ_z	−2.67	−2.24	−2.00	−1.915(1)[j]
	Θ_{zz}	−8.07	−7.91	−7.52	−7.0(3.3)[k]
H_2O	μ_z	−7.29	−6.61	−6.20	−6.16(2)[l]
	Θ_{xx}	−7.48			−8.34(7)[j]
	Θ_{yy}	7.75	8.53	8.52	8.77(7)[j]
	Θ_{zz}	−0.27			−0.43(10)[j]
H_2S	μ_z	−4.59	−3.64	−3.46	−3.25(17)[n]
	Θ_{xx}	−12.48	−13.02	−11.58	
	Θ_{yy}	9.38			
	Θ_{zz}	3.10			

[a] All calculations are at the molecular geometries of Feller et al.; *z* is the principal axis and the heavier atom in each case is along +*z*; C_{2v} molecules lie in the *yz* plane. All quantities in SI units (i.e. $\mu/10^{-30}$ C m; $\Theta/10^{-40}$ C m^2; see Table I for conversion factors). [b] Reference 53. [c] Reference 48. [d] Meerts, W. L.; De Leeuw, F. H.; Dymanus, A. *Chem. Phys.* **1977**, *22*, 319–324. [e] Muenter, J. S. *J. Chem. Phys.* **1972**, *56*, 5409–5412. [f] De Leeuw, F. H.; Dymanus, A. *J. Mol. Spectrosc.* **1973**, *48*, 427–445. [g] Kaiser, E. W. *J. Chem. Phys.* **1970**, *53*, 1686–1703. [h] Marshall, M. D.; Muenter, J. S. *J. Mol. Spectrosc.* **1981**, *85*, 322–326. [i] Kukolich, S. G. *Chem. Phys. Lett.* **1970**, *5*, 401–404. [j] Davies, P. B.; Neuman, R. M.; Wofsy, S. C.; Klemperer, W. *J. Chem. Phys.* **1971**, *55*, 3564–3568. [k] Kukolich, S. G.; Flygare, W. H. *Chem. Phys. Lett.* **1970**, *7*, 43–46. [l] Dyke, T. R.; Muenter, J. S. *J. Chem. Phys.* **1973**, *59*, 3125–3127. [m] Reference 63. [n] Huiszoon, C.; Dymanus, A. *Physica* **1965**, *31*, 1049–1052.

We see from the limited comparison in Table II that although the SCF/6-31G** results are generally inferior to the benchmark results, the difference for quadrupole moments is quite small, and the mean absolute deviation from experiment is slightly less than 1.0 × 10^{-40} C m^2, or of the order of typical experimental errors in Θ reported for most molecules (see the discussion above). We can therefore expect that this modest model will provide realistic estimates of quadrupole and second moments for the much larger systems presented in the following sections. It is also worthwhile noting from Table II that, as expected, the SCF/6-31G** model yields exaggerated predictions of molecular polarity; the anomalous case of CO has been widely discussed in the literature.

IV. X-ray Diffraction Methods for Obtaining Electric Moments

The determination of reliable molecular electron distributions from X-ray diffraction data is now a mature science. The first careful and accurate studies specifically targeted at the electron density were performed in the mid 1960s, and the first attempts to extract molecular properties date back to 1970. Many review articles have been published since then on the general principles involved and more specifically on the extraction of a wide range of electrostatic properties from the X-ray diffraction experiment. The reader is referred to those by Stewart et al.,[83-86] Coppens et al.,[31,87-92] Hirshfeld,[93,94] and Craven.[95,96] In particular the contributions from Coppens,[91] Coppens and Feil,[92] and Hirshfeld[94] are indicative of the more recent developments.

Only a small fraction of work in the field has been devoted to the extraction of electric moments. Two methods have principally been employed in the past, the rigid pseudoatom (or multipole) refinement, and direct integration of the electron density, and of these the latter has had limited application. In this section we discuss both, concentrating largely on the multipole refinement as that introduces most of the necessary concepts and ending with a brief discussion of error estimates. We make no attempt to be comprehensive in our presentation or discussion of the details pertinent to the various methods. That material is beyond the scope of this review and has been treated in great depth in the articles cited above.

A. Experimental Considerations

The time scale for the X-ray diffraction experiment is long compared to the duration of nuclear vibrations. Because of this, and the fact that the X-rays are scattered by electrons (and not nuclei), the measurement of the intensities of elastically scattered X-rays is a probe of the thermodynamic average electron density. The structure factor central to X-ray crystallography is the Fourier transform of this average electron density

$$F(\mathbf{S}) = \int_{\text{unit cell}} \bar{\rho}(\mathbf{r}) \exp(\mathrm{i}\mathbf{S}\cdot\mathbf{r})\, \mathrm{d}\mathbf{r} \qquad (15)$$

where $\mathbf{S}$ is the scattering vector, $|\mathbf{S}| = 4\pi \sin\theta/\lambda$, θ is the Bragg angle, and λ is the wavelength of the X-rays. Very broadly speaking this structure factor is directly related to the observed intensity

$$I(\mathbf{S}) \propto |F(\mathbf{S})|^2 \qquad (16)$$

It is worthwhile noting that the *everyday* use of these expressions relies largely upon the validity of the Born–Oppenheimer approximation, the assumption of a harmonic potential for the nuclei (although anharmonic potentials are increasingly common), and factorization of $\bar{\rho}(\mathbf{r})$ into nucleus-centered electron density functions (or pseudoatoms), each of which is assumed to follow the motion of the nucleus on which it is centered. Hence we have what is known as the rigid pseudoatom model, which underlies both the routine structural and the less routine charge density analysis of X-ray diffraction data. The details of the derivation have been most recently summarized by Stewart[97] and by Stewart and Feil.[98]

The determination of reliable electron distributions from crystals therefore relies upon the careful collection of reasonably large sets of intensities, $I(\mathbf{S})$. As discussed by Coppens and Feil[92] the best data sets currently collected on four-circle diffractometers display agreement between intensities of symmetry related reflections of 1–2%. This is one necessary requirement for the successful determination of $\bar{\rho}(\mathbf{r})$; others include careful attention to experimental effects such as extinction, multiple scattering, absorption, temperature of the data collection, reduction of the data to an absolute scale and, if at all possible, collection of a separate set of neutron diffraction data at the same temperature in order to more precisely determine thermal motion parameters and position coordinates, particularly of hydrogen atoms. The detailed experimental requirements for electron density analysis have been reviewed by Rees,[99] Lehmann,[100] and most recently by Blessing and Lecomte,[101] Fuess,[102] and Seiler.[103]

Table III summarizes the characteristics of the X-ray and neutron data sets upon which the dipole and quadrupole moment results discussed below are based. In the table we denote the data type as X or X + N, with obvious meaning. Other useful characteristics of the diffraction data are the maximum resolution of the X-ray data set, $(\sin\theta/\lambda)_{\max}$, the temperature at which the data was collected (generally the lower the temperature the smaller the effects of thermal motion), and the wavelength of the X-radiation used. Generally $(\sin\theta/\lambda)_{\max}$ should exceed 1.0 Å^{-1} in order to adequately resolve sharp features of $\rho(\mathbf{r})$, which implies the use of radiation of wavelength shorter than 1.0 Å (i.e. Mo or Ag X-ray tubes).

B. Rigid Pseudoatom Refinement

The multipole refinement of the electron distribution in crystals is a logical extension of the spherical atom approximation, which can be traced back to Debye who (in 1930!) speculated that the experimental determination of deviations from a simple spherical atomic model would produce information about the electron redistribution upon bonding.[156] The model (calculated) unit cell structure factor $F^{\mathrm{c}}(\mathbf{S})$ is expressed as a sum of pseudoatom contributions

$$F^{\mathrm{c}}(\mathbf{S}) = \sum_{\text{atoms } a} f_{\mathrm{a}}(\mathbf{S}) \exp(-2\pi \mathrm{i}\mathbf{S}\cdot\mathbf{r}_a) T_a(\mathbf{S}) \qquad (17)$$

where $f_{\mathrm{a}}(\mathbf{S})$ is a generalized atomic scattering factor and $T_{\mathrm{a}}(\mathbf{S})$ is (usually) an anisotropic temperature factor, the Fourier transform of the nuclear probability density function for nucleus a. It is worth emphasizing that the product $f_{\mathrm{a}}(\mathbf{S}) T_{\mathrm{a}}(\mathbf{S})$ represents the Fourier transform of a *mean thermal* electron density function for pseudoatom a. For the purposes of multipole refinement, the pseudoatom scattering factor $f_{\mathrm{a}}(\mathbf{S})$ is written as an expansion in radial and angular functions:

$$f_a(\mathbf{S}) = \sum_l \sum_m i^l f_{a,lm\pm}(S) A_{lm\pm}(\theta_S, \phi_S) \qquad (18)$$

The inverse Fourier transform of $f_a(\mathbf{S})$ is the pseudoatom electron density $\rho_a(\mathbf{r}_a)$

$$\rho_a(\mathbf{r}_a) = \sum_l \sum_m \rho_{a,lm\pm}(r_a) A_{lm\pm}(\theta_a, \phi_a) \qquad (19)$$

where $A_{lm\pm}(\theta_a,\phi_a)$ are usually, but not necessarily, real

Table III. Summary of X-ray and Neutron Diffraction Data Sets for which Electric Moment Results Are Discussed in the Text[a]

molecule	data type	$(\sin\theta/\lambda)_{max}$ (Å^{-1})	T (K)	ref(s)
Cl_2 chlorine	X	1.15	90	104
H_2O	X + N^b	1.15	92	105
water	X^b	1.37	97	106
	X + N^c	1.20	100	33
	X + N^d	1.15	120	107
	X + N^e	0.85	120	108
	X + N^f	1.32	120	109,110
	X^g	0.99	123	111
	X^h	0.65	123	111
H_3NO_3S sulfamic acid (1)	X + N	1.23	78	30
$H_{12}N_3B_3$ cyclotriborazane (2)	X	0.55	298	112
CH_2N_2 cyanamide (3)	X + N^i	1.08	100	113
CH_3NO formamide (4)	X	1.05	90	114
CH_4N_2O urea (5)	X + N	1.15	123	115,116
CH_4N_2S thiourea	X^j	0.90	298	117
C_2H_2 acetylene	X	0.80	141	118
C_2H_4 ethylene	X	1.07	85	119
$C_2H_4N_4$ 2-cyanoguanidine (6)	X	1.38	83	120
C_2H_5NO acetamide (7)	X^k	1.08	123	121
$C_2H_8NO_4P$ phosphorylethanolamine (8)	X + N	1.30	123	122,123
$C_3H_2N_2O_2S$ 2,5-diaza-1,6-dioxa-6a-thiapentalene (9)	X	1.25	11	124
$C_3H_2N_2O_3$	X + N	1.30	123	125
parabanic acid (10)	X + N	1.0	298	126
	X^j	0.90	298	117
$C_3H_3N_3$ *s*-triazine (11)	X + N	1.0	298	127
$C_3H_4N_2$ imidazole (12)	X + N	1.30	103	128,129
$C_3H_7NO_2$ L-alanine (13)	X	1.08	23	130
$C_4H_2N_2O_4$ alloxan (14)	X + N	1.15	123	131
$C_4H_4N_2$ pyrazine (15)	X	1.00	184	132
$C_4H_4N_2O_2$ uracil (16)	X	0.90	298	133
$C_4H_5N_3O$	X + N^b	1.15	82	105,134
cytosine (17)	X^b	1.37	97	106
$C_4H_8N_2O_3$ glycylglycine (18)	X + N	1.07	82	135,136
$C_4H_9NO_2$ γ-aminobutyric acid (19)	X + N	1.30	122	137,138
$C_5H_4N_2O_3$ *p*-nitropyridine *N*-oxide (20)	X + N	1.00	30	139,140
$C_5H_6N_2O_2$ 1-methyluracil	X + N	1.08	123	141,142
$C_6H_6N_2O_3$ 3-methyl-*p*-nitropyridine *N*-oxide	X + N	1.15	106	143
C_6H_6 benzene	X + N	1.30	123	144,145
$C_6H_7N_5$ 9-methyladenine (21)	X + N	1.00	126	146,147
$C_8N_2F_4$ *p*-dicyanotetrafluorobenzene	X	1.15	98	148
$C_8H_5N_3$ pyridinium dicyanomethylide (22)	X + N	1.06	118	149,150
$C_8H_{12}N_2O_3$ barbital (23)	X + N	1.08	198	151,152
$C_9H_6CrO_3$ benzenechromium tricarbonyl	X + N	0.99	78	153
$C_9H_{13}N_3O_5$ cytidine	X	0.99	123	111
$C_9H_{14}N_3O_7P$ deoxycytidine 5′-monophosphate	X	0.99	123	111
$C_{10}H_{13}N_5O_4$ deoxyadenosine	X	0.99	123	111
$C_{10}H_{13}N_5O_4$	X + N	1.1	123	154,155
adenosine	X	0.99	123	111
$C_{10}H_{14}N_2O_5$ deoxythymidine	X	0.99	123	111

[a] X refers to X-ray data only, X + N to X-ray and neutron diffraction data collected at the same temperature in a joint study. $(\sin\theta/\lambda)_{max}$ refers to the X-ray data set only. [b] Cytosine monohydrate. [c] Oxalic acid dihydrate. [d] Magnesium sulfite hexahydrate. [e] Magnesium thiosulfate hexahydrate. [f] Sodium hydrogen oxalate monohydrate. [g] Deoxycytidine 5′-monophosphate monohydrate and deoxyadenosine monohydrate. [h] Disodium guanosine 5′-monophosphate heptahydrate. [i] 1:2 complex of 18-crown-6 and cyanamide. [j] 1:1 complex of thiourea and parabanic acid. [k] 1:1 complex of acetamide and allenedicarboxylic acid.

surface harmonics in the spherical coordinate angles about a, and the radial density $\rho_{a,lm\pm}(r_a)$ is the Fourier–Bessel transform of $f_{a,lm\pm}(S)$. The pseudoatom electron density functions $\rho_a(\mathbf{r}_a)$ may be placed at their associated origins and then summed to form the electron distribution of a fragment, a molecule, or even the crystal.

Conventionally the set of model structure factors, $F^c(\mathbf{S})$, are optimized with respect to various population and radial parameters in the electronic model, and position and thermal parameters for the nuclei, using nonlinear least squares. This is done by minimization of

$$\epsilon = \sum_{\mathbf{S}} [|F^o(\mathbf{S})|^m - |F^c(\mathbf{S})|^m]^2 \qquad (20)$$

where the sum extends over all observed data, $F^o(\mathbf{S})$, and m is usually 1 or 2. There are currently a number of computer programs available for least squares multipole refinements of X-ray data, including LSEXP,[157,158] MOLLY,[159] POP,[160] and VALRAY.[161,162] The programs are similar in broad objectives but, like ab initio quantum chemical packages, differ in many subtle ways including the use of either spherical harmonics or cosine functions, and Slater-type or Gaussian radial functions. The results obtained by the various models are essentially the same, and have been compared in detail by simultaneous application to several data sets by Baert et al.[149] and more recently by Lecomte.[163]

The computation of electric moments for molecules consisting of a sum of pseudoatom electron densities is quite straightforward and has been discussed in detail by Coppens et al.[88] and Spackman et al.[164] We give an example here taken from the latter work, as it serves to illustrate in a more tangible fashion the workings of the multipole model. The pseudoatom electron density in eq 19 can be written in the POP or VALRAY models as

$$\rho(\mathbf{r}) = \rho_{\mathrm{at}}(r) + \sum_{l}^{L}\sum_{m=0}^{l} c_{lm\pm} R_l(r) y_{lm\pm}(\theta,\phi) \qquad (21)$$

where $\rho_{\mathrm{at}}(r)$ is a spherical atom electron density. The remaining terms describe the asphericity of the pseudoatom, with weights $c_{lm\pm}$ determined by the least-squares procedure. Least-squares fitting also provides $\sigma(c_{lm\pm})$ from which the errors in derived electric moments can be estimated. The radial functions in eq 21 are given by

$$R_l(r) = (4\pi)^{-1}\frac{\alpha^{n+3}}{(n+2)!} r^n \exp(-\alpha r) \qquad (22)$$

The angular functions are orthonormal spherical harmonics, which makes it straightforward to derive expectation values (atomic moments) of the form $\langle r^l y_{lm\pm}(\theta,\phi)\rangle$:

$$\begin{aligned} -\int r^l y_{lm\pm}(\theta,\phi)\rho(\mathbf{r})\,\mathrm{d}\mathbf{r} &= -c_{lm\pm}\int_0^\infty r^{l+2}R_l(r)\,\mathrm{d}r \int\int [y_{lm\pm}(\theta,\phi)]^2 \sin\theta\,\mathrm{d}\theta\,\mathrm{d}\phi \\ &= -c_{lm\pm}\frac{(n+l+2)!}{(n+2)!}\frac{(1+\delta_{m,0})}{\alpha^l(4l+2)}\frac{(l+m)!}{(l-m)!} \qquad (23) \end{aligned}$$

where the minus sign arises because the electron density is conventionally positive but possesses a negative charge. The nuclear charges are incorporated into the monopole term, which then represents the net pseudoatomic charge. For computation of molecular moments the point charges should be rescaled to produce a neutral molecule. This procedure is seldom of consequence as the rescaling factor is typically very close to unity, but it avoids introducing an unrealistic origin dependence for the moments. The molecular dipole moment is expressed as a sum of atomic dipoles plus atomic charges multiplied by distance, the quadrupole moment as a sum of atomic quadrupoles, dipoles multiplied by distance and charges multiplied by distance squared. For example for the dipole moment term μ_z

$$\mu_z = \sum_a [\mu_{a,z} + z_a q_a] \qquad (24)$$

and for the *zz* component of the quadrupole moment

$$\begin{aligned} \Theta_{zz} = \sum_a \Theta_{a,zz} + {}^1/_2\sum_a [2z_a\mu_{a,z} - x_a\mu_{a,x} - y_a\mu_{a,y}] &+ \\ {}^1/_2\sum_a [2{z_a}^2 q_a - {x_a}^2 q_a - {y_a}^2 q_a] & \qquad (25) \end{aligned}$$

Expressions in this form for molecular dipole and quadrupole moments appear to have been originally given by Stewart.[165]

The multipole refinement strategy generally has several objectives. Prime among these is the deconvolution of the electron distribution from its thermal motion to obtain a static picture of $\rho(\mathbf{r})$. It may in fact be more appropriate not to undertake this deconvolution, but rather to determine the moments of the mean thermal charge distribution. Although this has not been attempted to date, it would seem worthy of future attention (see below). An added advantage of the multipole refinement approach is that the resulting set of pseudoatoms can be used to build up the static electron distribution at apparent infinite resolution. This is not possible with a Fourier series construction, the inverse of eq 15, as the resolution of the data in reciprocal space (i.e. S space) is limited by the wavelength of the radiation, $\sin\theta/\lambda < \lambda^{-1}$. However, despite the ability of the multipole model to obtain a static, parametric representation of $\rho(\mathbf{r})$ for a molecule, it should be kept in mind that this has been extracted from its crystalline environment and hence necessarily contains information pertinent to that environment. Thus a urea molecule will surely display evidence of its participation in four hydrogen bonds in the crystal, and a benzene molecule should be expected to show a small, and possibly significant, deviation from the result expected for an isolated molecule. In this sense caution should be exercised when comparing diffraction results for molecular moments with those obtained for a free molecule by other techniques. We will see that this is the case below.

To facilitate a compact discussion of results in section V it is useful to distinguish between several commonly used variants of the multipole refinement model, in much the same way that ab initio calculations are categorized into minimal basis, double-ζ, DZP and so forth. The simplest of these are monopole models, where only spherical terms are included in the multipole expansion of the pseudoatom electron density. The earliest of these was the *L*-shell projection method of Stewart,[12] and the most widely applied is the κ-refinement procedure of Coppens et al.[166] Any multipole refinement restricted to monopole functions is formally akin to least-squares fitting of the electrostatic potential in the crystal by a point charge model, and hence monopole models are quite capable of yielding excellent estimates of molecular dipole and quadrupole moments, as we shall see below. More complex than the monopole model, a typical multipole refinement for an organic molecule generally includes functions up to the dipole or quadrupole level on H atoms and up to the octopole or hexadecapole level on C, N, or O.

C. Direct Integration Methods

Direct integration methods for the determination of electric moments of molecules in crystals originated in the work by Coppens and Hamilton on the integration of electron density within a parallelepiped in a crystal.[167] Direct integration for molecular moments has since been discussed in detail by Coppens and co-workers,[88,168,169] but because of the limited number of applications only a brief outline will be given here to illustrate the method and to distinguish it from the multipole refinement procedure.

Properties dependent upon the electron distribution may be expressed in terms of the operator equation

$$\langle O(\mathbf{r})\rangle = \int_v O(\mathbf{r})\rho(\mathbf{r})\,\mathrm{d}\mathbf{r} \qquad (26)$$

where the integration is over the volume of interest, *v*, which may be the unit cell, or a volume defined by a molecule, ion or cluster, and $O(\mathbf{r})$ is an appropriate operator (1 for net charge, $\mathbf{r}$ for dipole moment etc.). When $\rho(\mathbf{r})$ is the electron distribution obtained from X-ray structure factors we can insert its Fourier expansion (the inverse of eq 15) to obtain

$$\langle O(\mathbf{r})\rangle = \frac{1}{V}\int_v O(\mathbf{r}) \sum_{\mathbf{S}} F^{\circ}(\mathbf{S}) \exp(2\pi i\mathbf{S}\cdot\mathbf{r})\, d\mathbf{r} \quad (27)$$

and the expectation value obtained in this fashion refers to a thermally averaged electron density, since eq 26 contains a sum over the observed structure factors. In practice the integration is performed over the deformation density, the difference between the electron density and a hypothetical model of independent spherical atoms, the so called IAM or promolecule, and the particular volume v is divided into smaller subunits of identical shape and orientation, generally parallelepipeds. Use of the deformation density in eq 27 suppresses series termination effects in the Fourier sums; the contribution from the promolecule is readily obtained directly.

The determination of molecular electric moments by direct integration techniques is critically dependent upon the definition of a molecular boundary. This may appear to be hopelessly arbitrary, but two sensible, and very different, choices have been employed:[170]

(i) *discrete boundary* (DB) partitioning defines the molecular volume in the manner of a generalized Wigner–Seitz cell,[171] which places the boundary surface in a sensible region of low electron density between molecules; and

(ii) *fuzzy boundary* (FB) partitioning, which is an extension of Hirshfeld's stockholder method,[34] where each point on the integration grid is weighted according to the individual promolecule contribution to the sum of all promolecules in the crystal. As we shall see below, in spite of the distinct differences between the direct integration approaches (which we will label DI-FB and DI-DB), they lead to rather similar results. Moss and Coppens[170] have also used both integration approaches to explore the application of the direct integration method to a formamide crystal composed of ab initio derived molecular electron densities (i.e. excluding hydrogen bonding perturbations). Their results suggest that the good agreement between experimental dipole moments obtained from the diffraction data and those determined by other methods seems to be fortuitous, an example of cancellation of errors, as correct dipole moments are only retrieved from the hypothetical crystal electron density when the cell dimensions are doubled (i.e. intermolecular distances increased substantially). The large body of results to be presented in the following section are at variance with this conclusion, as is a separate analysis of structure factors obtained from an ab initio wave function for formamide, discussed by Coppens and Stevens;[89] a reexamination of Moss and Coppens' model study would seem to be in order.

D. Estimates of Errors

Molecular moments obtained from X-ray diffraction data, like those from other experimental sources, are of greater value when accompanied by realistic error estimates. The error estimate for multipole refinement results, perhaps surprisingly, depends upon the choice of origin, even if μ, Θ, etc. are origin independent. To see this, consider the μ_z component of the dipole moment given by eq 24. Simple propagation of errors leads to the expression

$$\sigma^2(\mu_z) = \sum_a [\sigma^2(\mu_{a,z}) + z_a^{\,2}\sigma^2(q_a)] \quad (28)$$

where $\sigma^2(\mu_{a,z})$ and $\sigma^2(q_a)$ are readily obtainable from the least-squares procedure, and we have ignored experimental errors in position coordinates. (This assumption simplifies error analysis without compromise as relative errors in position coordinates are usually much smaller than relative errors in multipole model parameters.[86]) Clearly eq 28 depends upon our choice of origin; we recommend that the molecular center of mass be used as origin for the reporting of all molecular moments *and their errors* from diffraction data, and we adopt this convention as far as possible in the following section. This is not only conventional (for Θ) and convenient, but it also guarantees that since the center of mass lies within the molecular envelope, $\sigma(\Theta)$ will not become large and essentially meaningless.

Error estimates in quantities derived by direct integration depend solely upon the magnitude of the errors in the experimental structure factors, $\sigma[F^{\circ}(\mathbf{S})]$. Coppens et al.[88] provide details of the computation, but it appears to have been performed infrequently.

V. Diffraction Results

A. Dipole Moments

Diffraction estimates of the magnitude of the dipole moment, μ, for a large number of molecules are summarized in Table IV, where they are also compared with other experimental results and, where possible, with computed ab initio SCF/6-31G** values. We discuss each of the systems in Table VI in turn, then explore the possibility that the diffraction experiment is actually giving a quantitative estimate of dipole moment enhancement upon hydrogen bonding, and finally discuss the orientation of μ for a selection of molecules for which the dipole moment direction is accurately known from microwave studies in the gas phase or from ab initio theory. **Note**: To avoid repetition of unwieldy powers of 10, numerical results for dipole moments will be assumed to be in SI units in all discussion (i.e. must be multiplied by 10^{-30} C m). Structures for the compounds discussed in the following section are in Chart I.

1. Discussion of Results

a. Water. Most results so far reported for water pertain to a water molecule hydrogen bonded to either oxalic acid or cytosine in the crystal or bound to a cation such as Mg^{2+}. They usually possess a small net charge of up to several tenths of an electron, but in spite of this drawback, all estimates of μ in Table IV are sensible and, with the exception of those from Eisenstein[106] and the direct integration values from Bats and Fuess,[172] greater than the gas-phase microwave result. The values obtained via multipole refinement by Weber and Craven,[105] Stevens and Coppens,[33] Bats et al.[107,172] and Delaplane et al.[110] all agree well, coming as they do

Table IV. Diffraction Estimates of Dipole Moments Compared with Other Experimental Results, Where Available, and with ab Initio Theoretical Results[a]

molecule	diffraction results	other experiment or theory
H_2O water	7.7 (10), multipole[105] 5.3, multipole[106] 6.40 (17), DI-DB[33] 7.0 (7), multipole[33] 7.2 (5), multipole[107] 7.9 (5), multipole[107] 7.6–8.3 (5), monopole[172] 7.0–7.6 (5), monopole[172] 3.9–6.5, DI-DB[172] 8.13 (3), multipole[110] 6.5–8.9, monopole[111]	6.186 (1)/gas[173] 7.29/6-31G**
H_3NO_3S sulfamic acid (1)	32.7 (20), monopole[166] 33.0 (20), multipole[88]	34.0–44.4/solution[174] 29.97/6-31G**
$H_{12}N_3B_3$ cyclotriborazane (2)	13.7 (13), monopole[112]	9.0 (4)/solution[175] 12.98/6-31G**
CH_2N_2 cyanamide (3)	18.5, multipole[113]	13.3–15.1/solution[176] 16.26/6-31G**
CH_3NO formamide (4)	14.6 (17), monopole[166] 16.1 (17), multipole[166] 16.5, DI-DB[170] 13.4, DI-FB[170]	12.4 (2)/gas[177] 12.8 (1)/solution[178] 14.18/6-31G**
CH_4N_2O urea (5)	18.0 (17), multipole[115] 19.0 (17), multipole[115]	12.8 (1)/gas[179] 15.2/solution[180] 15.5/crystal[181] 17.06/6-31G**
CH_4N_2S thiourea	18.0 (83), multipole[117]	16.3/solution[180] 22.31/6-31G**
$C_2H_4N_4$ 2-cyanoguanidine (6)	22.6, multipole[120] 37.5, multipole[120]	27.2/solution[176] 30.27/6-31G**
C_2H_5NO acetamide (7)	16.5, multipole[182]	12.3 (1)/gas[183] 12.9 (1)/solution[178] 15.16/6-31G**
$C_2H_8NO_4P$ phosphorylethanol amine (8)	43 (7), multipole[122]	72.82/6-31G**
$C_3H_2N_2O_2S$ 2,5-diaza-1,6-dioxa-6a-thiapentalene (9)	7 (3), multipole[124] 44.7, monopole[111]	9.61 (7)/solution[184]
$C_3H_2N_2O_3$ parabanic acid (10)	7.7 (10), multipole[125] 11.7 (60), multipole[126] 15.7 (70), multipole[117]	8.92/6-31G**
$C_3H_4N_2$ imidazole (12)	16.0 (20), multipole[129]	12.2 (2)/gas[185] 13.2 (1)/solution[186]
$C_3H_7NO_2$ L-alanine (13)	43.0 (23), multipole[130]	41.0/solution[187] 41.4/6-31G** [130]
$C_4H_2N_2O_4$ alloxan (14)	0.7 (33), multipole[131]	9.93/6-31G**
$C_4H_4N_2O_2$ uracil (16)	13.3 (43), monopole[12,83,188] 14.7 (43), monopole[189]	13.9 (1)/solution[13] 16.22/6-31G**
$C_4N_5N_3O$ cytosine (17)	26.7 (47), multipole[134] 19.5, multipole[106]	23.3 (est)/solution[190] 27.47/6-31G**
$C_4H_8N_2O_3$ glycylglycine (18)	80.4 (28), monopole[166]	91–93/solution[191]
$C_4H_9NO_2$ γ-aminobutyric acid (19)	43.4 (33), multipole[137]	55.7–67.4/solution[192,193] 67.00/6-31G**
$C_5H_4N_2O_3$ *p*-nitropyridine *N*-oxide (20)	1.3 (33), monopole[166]	2.3 (1)/solution[194] 1.00/6-31G**
$C_5H_6N_2O_2$ 1-methyluracil	14.7 (73), multipole[141] 21.3 (90), multipole[141]	13.9 (1)/solution[13] 18.27/6-31G**
$C_6H_6N_2O_3$ 3-methyl-*p*-nitropyridine *N*-oxide	5.3 (43), monopole[143] 11.9 (47), monopole[143]	
$C_6H_7N_5$ 9-methyladenine (21)	6.0 (33), multipole[147] 8.0, multipole[106]	10.8 (7)/solution[195]
$C_8H_5N_3$ pyridinium dicyanomethylide (22)	62.7, multipole[149] 32.7, multipole[149] 20.0, multipole[149] 34.0, DI-FB 27.6, DI-DB	30.7/solution[196] 36.17/6-31G**
$C_8H_{12}N_2O_3$ barbital (23)	2.3 (40), multipole[151]	3.77 (3)/solution[197]
$C_9H_6CrO_3$ benzenechromium tricarbonyl	18.3 (83), monopole[153]	16.8/solution[198]
$C_9H_{13}N_3O_5$ cytidine	52.0, monopole[111]	
$C_9H_{14}N_3O_7P$ deoxycytidine 5′-monophosphate	50.7, monopole[111]	
$C_{10}H_{13}N_5O_3$ deoxyadenosine		
$C_{10}H_{13}N_5O_4$ adenosine	25.7 (170), multipole[155] 8.0, monopole[111]	
$C_{10}H_{14}N_2O_5$ deoxythymidine	49.7, monopole[111]	

[a] All quantities in SI units (i.e. $\mu/10^{-30}$ C m; see Table I for conversion factors). Other experimental results are labeled as either "gas" (i.e. microwave), "solution" (i.e. benzene, dioxane, or aqueous solution), or "crystal"; see text for details. 6-31G** ab initio results have been obtained at the SCF level, generally at the neutron crystal geometry.

from quite different crystalline hydrates. It is significant that the results obtained by Bats and Fuess in a κ-refinement study of hydrated magnesium thiosulfate are in good agreement with values obtained from multipole refinements of the same data. The direct integration result of 6.40 (17), obtained for water in oxalic acid dihydrate, is also in accord with those values, but Eisenstein's value of 5.3 and the DI-DB values from Bats and Fuess in the range 3.9 to 6.5 are somewhat lower. Although obtained from a multipole refinement, Eisenstein's value has been treated in a different manner to the other multipole results reported for water in Table IV. Instead of constructing a pseudomolecule removed from the crystal by summing pseudoatom fragments, Eisenstein performed a partitioning of the pseudocrystal electron density based on Hirshfeld's stockholder method.[34] This technique has also been used in analyses of other systems (see cytosine, adenine, 2-cyanoguanidine, and pyridinium dicyanomethylide below), and generally yields a lower estimate of the dipole moment. The DI-DB results obtained for the water molecules in hydrated magnesium thiosulfate clearly display a systematic dependence upon the radii used to define the molecular boundaries.

The monopole results in the range 6.5–8.9 in Table IV have been deduced from κ-refined charges obtained by Pearlman and Kim[111] for water molecules in several nucleosides and nucleotides. In spite of the lack of neutron data to locate the hydrogen atom positions in those studies, the point charges obtained clearly yield sensible dipole moments for the water molecules and even suggest an enhancement over the isolated molecule value.

b. Sulfamic Acid (1). The κ-refinement (monopole) and multipole results are in agreement, and both are close to the smaller of the results obtained in various nonaqueous solutions by Sears, Fortune, and Blumenshine.[174] Sears et al. also attempted to correct their results for solvent effects, obtaining values in the range 22.0–26.5 as estimated gas-phase dipole moments, which are in better accord with the diffraction results and the SCF/6-31G** result in Table IV, especially if we take into account the general systematic overestimate of μ at this level of theory.

c. Cyclotriborazane (2). The X-ray data set of Corfield and Shore[112] is among the least accurate of those reported in this work, with a resolution of only 0.55 Å^{-1} and collected at room temperature. Never-

Chart I[a]

1 sulfamic acid

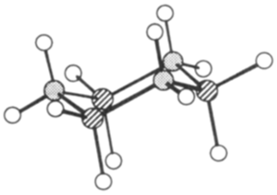

2 cyclotriborazane

3 cyanamide

4 formamide

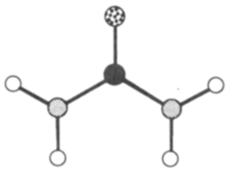

5 urea

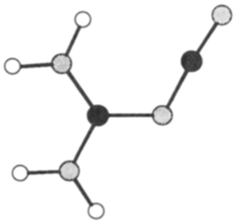

6 2-cyanoguanidine

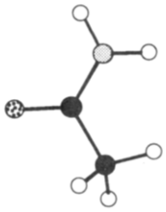

7 acetamide

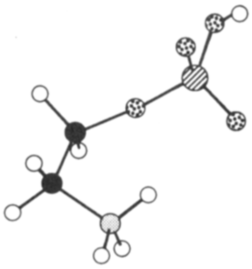

8 phosphorylethanolamine

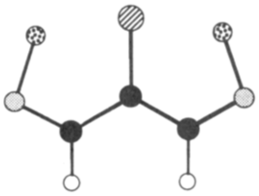

9 2,5-diaza-1,6-dioxa-6a-thiapentalene

10 parabanic acid

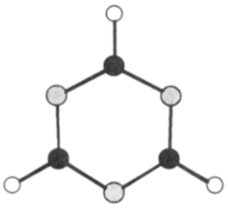

11 *s*-triazine

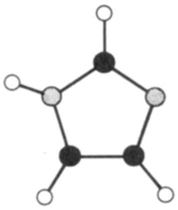

12 imidazole

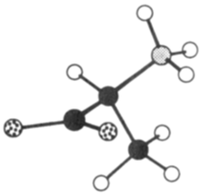

13 L-alanine

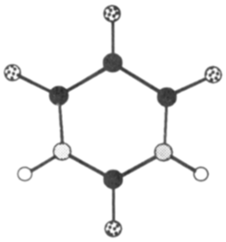

14 alloxan

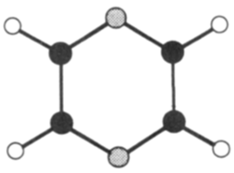

15 pyrazine

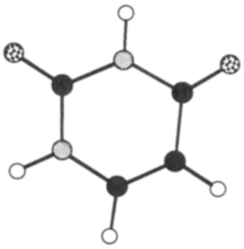

16 uracil

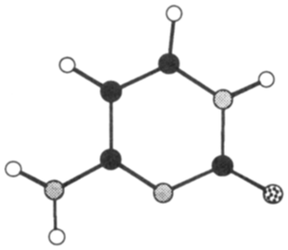

17 cytosine

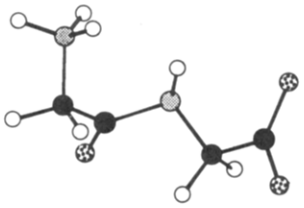

18 glycylglycine

19 γ-aminobutyric acid

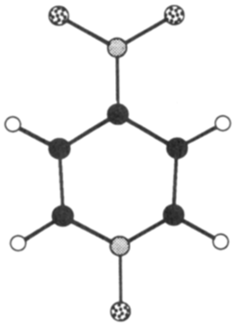

20 *p*-nitropyridine *N*-oxide

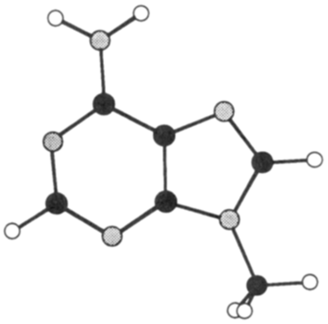

21 9-methyladenine

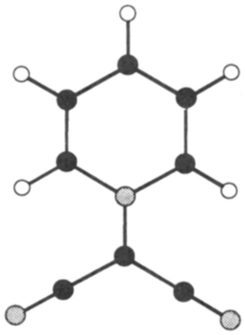

22 pyridinium dicyanomethylide

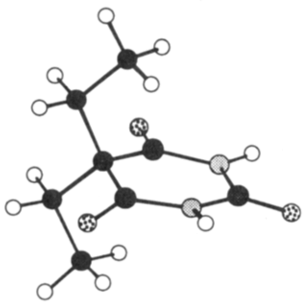

23 barbital

---

[a] The less common molecules encountered in the text are accompanied by one of the structural formulas 1–23. Atom type is coded by the fill pattern of the circles: ●, carbon; ◍, nitrogen; ⊛, oxygen; ○, hydrogen; ▨, boron, sulfur, or phosphorus. The size of each circle has no particular significance.

theless the data is clearly adequate to define the direction and magnitude of the dipole moment. Corfield and Shore estimated atomic charges by performing an L-shell projection[12] and reported atomic charges and molecular dipole moments from nine different strategies. An average of these, 9.7 (110), was compared with a solution measurement in dioxane [9.0 (4)] by Leavers and Taylor.[175] Upon close examination of the individual refinements reported by Corfield and Shore it is clear that three of them (A, B, and C in their Table I) did not include refinement of position or thermal parameters and yield dipole moments of opposite sign to those from other refinements in the table. For a sensible comparison with more recent monopole refinement strategies we have reported the value from their refinement G in Table IV, 13.7 (13), which we expect is more realistic, and as observed in many other cases below exceeds the solution result.

d. Cyanamide (**3**). In the recent combined X-ray and neutron study of the 1:2 18-crown-6–cyanamide complex at 100 K, Koritsanszky et al.[113] report a dipole moment for cyanamide and for segments of the polyether from a multipole refinement. The complex clearly contains an inversion center relating the two identical cyanamide guest molecules, and as a consequence the crown ether host cannot possess a net dipole moment. The dipole moment for cyanamide reported by Koritsanszky et al., 18.5, is substantially larger than the values of 13.3 and 15.1, in benzene and dioxane solutions, respectively, reported by Schneider.[176] Part of this difference can be ascribed to the distortion of the molecule in the complex compared to the gas-phase geometry: the 6-31G** dipole moment of 16.26 given in Table IV refers to the neutron geometry in the crown ether complex, whereas a calculation with the isolated molecule structure[199] yields 15.60. Tyler et al.[199] also obtained a value for the component of the dipole moment along the major inertial axis (essentially along the N–C–N backbone) from the microwave Stark effect; their result implies that the dipole moment of an isolated molecule would be slightly greater than 14.4 (3).

e. Formamide (**4**). The X-ray data on formamide collected at 90 K[114] has been used to test all techniques described in section IV for estimating electric moments from diffraction data. It is particularly significant that all methods yield essentially the same result: the values range from 13.4 to 16.5, each with an error of the order of 1.7. (Although not all were reported with associated errors, we can safely assume them to be of a similar magnitude to those given in Table IV.) Again, we note that these estimates of μ from diffraction data are greater than that measured for an isolated molecule, a matter which we will discuss separately in some detail below.

f. Urea (**5**). The two multipole values reported for urea derive from two similar multipole refinements performed by Swaminathan et al.[115] The apparent enhancement of the dipole moment over that observed in the gas phase is very large in this instance, perhaps attributable to the high symmetry of the nearest-neighbor environment of each molecule in the crystal and the fact that each participates in four hydrogen bonds. The value of 15.5 obtained by Lefebvre[181] from lattice-dynamical modeling of phonon dispersion curves in crystalline urea is also significantly greater than the isolated molecule value. An earlier lattice-dynamical study by Lefebvre[200] using a hydrogen bond and dipole–dipole potential inferred a value of 18.5 for the dipole moment of urea in the crystal, in excellent agreement with the multipole results of Swaminathan et al.

g. Thiourea. The room-temperature X-ray data set of Weber and Craven[117] on the thiourea–parabanic acid complex is more modest than most others included in Table IV, yet the diffraction experiment clearly yields sensible quantitative information about the polarity of both molecules in the crystal and their interactions. The dipole moment obtained for thiourea is similar to that of urea and again greater than that measured for an isolated molecule; the lesser precision of the room-temperature data in this case is reflected in the very large error (46%) reported for μ. Spackman, Weber, and Craven[164] have used this data, among others, to derive intermolecular interaction energies in the crystal and have concluded that data sets of this quality are simply not adequate for precise quantitative determination of electric properties and energies. Nevertheless much can still be learned about the nature of the interactions in the crystal, and molecular dipole moments at this level of precision are good enough to rationalize crystal packing arrangements in many instances.

h. 2-Cyanoguanidine (**6**). This high-resolution, low-temperature X-ray data on **6** (dicyandiamide) has been analyzed by Hirshfeld and Hope[120] using Hirshfeld's multipole model.[157] The resulting static electron distribution has been treated in two distinct ways: one involved simply summing the pseudoatom electron density functions to form a pseudomolecule extracted from the crystal in the manner of most other multipole determinations of μ in Table IV. The other treatment consists of constructing a cluster, comprising a central molecule and its immediate neighbors out to an atom–atom separation of 5 Å, and then partitioning the electron density of the cluster using Hirshfeld's stockholder method.[34] The fragments belonging to the central molecule were then summed to obtain molecular electric moments. This is the same approach pursued by Eisenstein in her study of cytosine monohydrate.[106] The two treatments *of the same static electron distribution in the crystal* yield quite different results; the simple summation of pseudoatom fragments giving a value of 37.5 for 2-cyanoguanidine, while the stockholder partitioning yields a much lower estimate of 22.6. No experimental errors were quoted by Hirshfeld and Hope. Both the experimental value of 27.2 obtained by Schneider[176] from dioxane solution and the SCF/6-31G** result of 30.27 suggest a value of approximately 26 for an isolated molecule. Hirshfeld and Hope have discussed the difference between the two treatments of multipole-refined electron distributions and conclude that the Hirshfeld partitioning of the model electron density in the crystal tends to produce lower bounds to electric moments as it allows a mutual cancellation of positive and negative deformation functions centered on neighboring molecules. The low value for μ obtained for water by Eisenstein lends support to this conclusion, as do several other studies described later in this section.

i. Acetamide (**7**). The diffraction estimate of 16.5 for the dipole moment of acetamide comes from a multipole refinement of the low-temperature X-ray data of Berkovitch-Yellin et al.[121] of the 1:1 complex of acetamide with allenedicarboxylic acid. It is substantially greater than the value of 12.3 observed in the gas phase[183] or that of 12.9 in dioxane.[178] Again it is tempting to attribute this enhancement to the effect of hydrogen bonding in the crystal, where acetamide molecules participate in two N—H···O=C hydrogen bonds to form cyclic dimers. In a separate study, Ruble, Wang, and Craven[201] have reported atomic charges obtained from an *L*-shell refinement procedure for a series of 1:1 crystal complexes of barbital, including acetamide. All X-ray data analyzed were modest (room temperature, Cu Kα) but can still be used to estimate dipole moments; for the acetamide–barbital complex a value of 14.8 (23) is obtained for the dipole moment of acetamide, in very good agreement with that obtained by Berkovitch–Yellin et al. Unfortunately not all molecular dipole moments obtained by Ruble et al. from these modest X-ray data sets are sensible, probably largely due to the lower resolution of the Cu data sets and problems associated with the much larger amplitudes of thermal motion of the molecules at room temperature.

j. Phosphorylethanolamine (*8*). This molecule comprises the polar head of some lipids and exists as a zwitterion in the crystal. The dipole moment has been obtained from a multipole refinement using low-temperature X-ray data in conjunction with neutron data,[122,123] and the value of 43 (7) so obtained reflects the strongly polar nature expected of the molecule. The ab initio value of 72.82 was obtained at the neutron-refined geometry and, as discussed earlier, is most likely to overestimate, by 10 to 20%, a value appropriate to an isolated molecule. No other experimental results seem to have been published.

k. 2,5-Diaza-1,6-dioxa-6a-thiapentalene (*9*). Fabius et al.[124] analyzed the very-low-temperature X-ray data on **9** using the Hansen and Coppens multipole formalism[159] in conjunction with neutron data collected at 122 K.[202] The results obtained were quantitatively different from an earlier X-ray study at 122 K[202] and reinforce the gains to be made by measuring X-ray diffraction intensities at cryogenic temperatures. The dipole moment derived from their multipole refinement, 7 (3), agrees well with a measurement of 9.61 (7) in dioxane solution.[184]

l. Parabanic Acid (*10*). The results for **10** (1*H*,3*H*-imidazoletrione) reported in Table IV derive from separate multipole refinements of room temperature X-ray data[126] and low-temperature X-ray and neutron data on the molecule[125] and also room temperature X-ray data on its 1:1 complex with thiourea.[117] The results of 7.7 (10) and 11.7 (60) obtained for the molecular crystal agree with one another, with the larger error (51%) quoted for the latter reflecting the lower precision of the room temperature data. That the more precise value is also more reasonable can be seen from the ab initio estimate of 8.92 at the neutron-refined geometry, a value we expect to overestimate the true isolated molecule result. The value of 15.7 (70) obtained for the thiourea complex at room temperature may reflect an enhanced polarity in the strongly hydrogen bonded environment of the complex, but the experimental error is considerable.

m. Imidazole (*12*). The multipole refinement result of 16.0 (20) obtained from low-temperature X-ray and neutron data by Epstein et al.[128,129] exceeds those reported in the gas phase and in dioxane solution. Curiously in this instance the ab initio value is less than the multipole refinement result, but still greater than the microwave measurement. The apparent enhancement of μ is in line with that observed above for similar hydrogen-bonded molecules.

n. L-*Alanine* (*13*). The results reported in Table IV were obtained from very-low-temperature (23 K) X-ray data collected by Destro, Marsh, and Bianchi.[203] Quite extraordinary care was taken in the data collection, with all intensities measured a total of three times. The data were analyzed with several variations of Stewart's multipole refinement strategy, yielding dipole moments in the narrow range 42.4 (23)–43.7 (23);[130] the mean of these is reported in Table IV. Such a large dipole moment is expected from the zwitterionic structure of the molecule in the crystal; a similar outcome was noted for phosphorylethanolamine (above) and is also observed for glycylglycine and γ-aminobutyric acid (see below). The diffraction estimate of μ is in accord with the ab initio SCF/6-31G** value of 41.4 obtained by Destro et al. and also with the value of 41.0 for a 1.0 M aqueous solution by Khanarian and Moore[187] (in that work the pH of the solution was near the isoelectric point for the amino acid, hence the zwitterion is the predominant species). There appear to be no measurements of μ in the gas phase or in nonaqueous solutions, but the dipole moment of an isolated molecule will most likely be substantially less than all of these results.

o. Alloxan (*14*). The crystal structure of **14** (2,4,5,6-(1*H*,3*H*)-pyrimidinetetrone) is unusual in that in spite of the presence of *only* N—H and C=O functional groups in the molecule, no strong hydrogen bonds are formed. Instead the crystal appears to derive much of its stability from short intermolecular C=O···C contacts, which are also observed in parabanic acid. The dipole moment obtained from a multipole refinement using low-temperature X-ray and neutron data[131] is essentially negligible, 0.7 (33). In contrast, the ab initio result, obtained using the neutron geometry, is 9.93, which is likely to be an overestimate, but clearly not by much for this effectively nondipolar molecule. There are no other experimental results for this curious molecule, although an INDO study of tautomers of **14**[204] (which reports an INDO dipole moment of 7.5) cites an experimental value of 7.00; this pertains to measurements in dioxane solution of alloxan monohydrate,[197] which is more closely related to barbituric acid, and quite different from the molecule studied by Swaminathan et al.

p. Uracil (*16*) *and 1-Methyluracil.* As discussed in the Introduction to this review, perhaps the first dipole moment reported from X-ray diffraction data was that of uracil, obtained from an *L*-shell monopole refinement by Stewart.[12] The room-temperature X-ray data collected by Stewart[133] is modest by modern standards, yet sufficient to reliably define the magnitude and direction of μ for **16**. Stewart's original result, 13.3 (4.3), has since been confirmed by a similar monopole refinement of the same data, which yielded 14.7 (4.3),[189] and a measurement in dioxane solution by Kulakowska et al.[13] which gave a value of 13.9 (1).

For 1-methyluracil, two low-temperature X-ray data sets[141] have been analyzed in conjunction with neutron data[142] using Stewart's model.[141] The results reported in Table IV are from refinements labeled II and IIv (both with the same X-ray data set) by Klooster et al. and agree with one another, and with the value obtained in dioxane solution, within the rather large errors reported. A dipole moment of 34.7 (80), significantly different from those in Table IV, was also reported by Klooster et al., from analysis of a separate low-temperature X-ray data set (labeled refinement I by Klooster et al.). There was, however, uncertainty in the temperature of that experiment (by approximately 20 K) which precluded use of the 123 K neutron results from McMullan and Craven;[142] position parameters for H atoms were taken from an earlier neutron study of 1-methylthymine and only isotropic thermal parameters were refined on H atoms, along with a more restricted multipole model. For these reasons the dipole moment from refinement I is unlikely to be as reliable as those reported in Table IV. This conclusion is supported by the SCF/6-31G** result of 18.27, which is more than likely a substantial overestimate of the isolated molecule value.

q. Cytosine (**17**). The multipole refinement values listed in Table IV are both derived from studies of cytosine monohydrate, and the relevant data have been discussed above in the context of μ for the water molecule. As observed for water, the result obtained by Eisenstein[106] via a Hirshfeld partitioning of the model electron density is much lower than that from a direct summation of pseudoatom moments. This would seem to clearly demonstrate a systematic difference between the results to be obtained from the two approaches. In this case the result of Weber and Craven[105] is more in line with the value of 23.3 estimated from solution measurements on substituted cytosines[190] and the present ab initio value of 27.47 obtained at the neutron geometry. Here, as for water and 2-cyanoguanidine, the summation of pseudoatom moments provides results which are both more in accord with the philosophy of the pseudoatom multipole refinement strategy, as well as in agreement with expectations based upon comparison of diffraction results for similar systems with other experimental and theoretical results.

r. Glycylglycine (**18**). Coppens et al.[166] have reported three slightly different sets of atomic charges from κ refinements using the low-temperature X-ray and neutron data of Kvick et al.[135,136] All yield dipole moments in essential agreement, and the weighted mean of 80.4 (28) is reported in Table IV. This value is less than the aqueous solution measurement of Sakellaridis and Karageorgopolous.[191]

s. γ-Aminobutyric Acid (**19**). The low-temperature X-ray and neutron data of Weber et al.[137,138] have been analyzed with Stewart's multipole model; the resulting dipole moment of 43.4 (33) is much as expected for a zwitterionic molecule such as this and is very reasonable considering the range of values (55.7 to 67.4) recorded in 1 M aqueous solution.[192,193] Pottel et al.[193] have also estimated a correction for solvent effects, obtaining values between 31.4 and 32.0 for an effective gas-phase dipole moment. This is probably a sensible result and reinforces the observation of enhanced dipole moments of these hydrogen-bonded molecules in the crystal.

t. p-Nitropyridine N-Oxide (**20**) *and 3-Methyl-p-nitropyridine N-Oxide*. The very small dipole moment of 1.3 (33) obtained by Coppens et al.[166] from a monopole refinement of very-low-temperature X-ray data for **20** is in excellent agreement with the measurement of 2.3 (1) in benzene solution by Katritzky et al.[194] and also the present 6-31G** value of 1.00 computed at the neutron geometry.

For the 3-methyl derivative, low-temperature X-ray and neutron data were collected by Baert et al.[143] as part of an investigation of molecules related to pyridine *N*-oxide for optoelectronics. These molecules display strong charge transfer, but the unsubstituted *p*-nitropyridine *N*-oxide crystallizes with a center of symmetry, hence the nonlinear second-order susceptibility vanishes; the 3-methyl derivative, on the other hand, crystallizes in the acentric space group $P2_12_12_1$. Baert et al. reported dipole moments obtained from κ-refinements using the X-ray data with varying constraints on position and thermal parameters of the H atoms. The value of 5.3 (43) (Table IV) results from use of neutron position and thermal parameters, while the larger result of 11.9 (47) was obtained by allowing the H-atom positions to vary. While these two dipole moment estimates are not significantly different, we would anticipate the replacement of a H atom by a methyl group to have a small effect on μ (for example at the SCF/6-31G** level μ(1-methyluracil) exceeds μ(uracil) by only 2.05 × 10^{-30} C m). Only the lower estimate is in accord with the results (X-ray, solution or ab initio) in Table IV for *p*-nitropyridine *N*-oxide. In addition Berthier et al.[205] have recently reported ab initio calculations of the dipole moment and polarizability of both of these molecules using two medium-sized basis sets. The dipole moment obtained with the larger basis set (basis II of Berthier et al.[205]) for the conformation observed in the crystal is 1.60 × 10^{-30} C m, in accord with the values given in Table IV for *p*-nitropyridine *N*-oxide and the lower of the two results for the 3-methyl derivative.

u. 9-Methyladenine (**21**). The low-temperature X-ray and neutron data sets[146,147] have been analyzed with Stewart's model by Craven and Benci[147] and with Hirshfeld's model by Eisenstein.[106] Both results are in agreement but this is the only instance where a stockholder partitioning of the model electron density in the crystal yields a higher value for μ than the direct summation of pseudoatom moments. We note however that the two refinements employed in each case are quite different (i.e. the two do not refer to different treatments of the same model electron density, as was the case for pyridinium dicyanomethylide), and the experimental error is large (55% in the only case where an error is cited). Nevertheless, both multipole refinement results are close to the measurement of 10.8 (7) in dioxane solution.[195] 9-Methyladenine is clearly only weakly dipolar (especially when compared to cytosine, another nucleic acid base), and this observation concurs with the estimate of −17 (3) kJ mol^{-1} for self-association of 9-ethyladenine in solution.[206]

v. Pyridinium Dicyanomethylide (**22**). Low-temperature X-ray data on **22** was analyzed by Baert et al.[149] using both the Hirshfeld pseudoatom model[157] and that adopted by Hansen and Coppens[159] as a test of the two refinement procedures. The results obtained from this study vary dramatically; the Hirshfeld model refinement yields both the highest value of 62.7 (from a direct summation of pseudoatom moments) and the lowest value of 20.0 (from a stockholder partitioning of the static model electron density in the crystal). In contrast to this is the more conventional multipole refinement strategy which yielded 32.7, in agreement with the value of 30.7 obtained by Treiner et al.[196] from studies of dipole association in dioxane solutions. A still lower result of 26.7 has been obtained in electrooptic studies by Varma and Groenen,[207] but this has been inferred from a value for the excited state. The results obtained by Moss and Coppens by direct integration of the X-ray data (34.0 for a fuzzy boundary; 27.6 for a discrete boundary) are in accord with the conventional multipole refinement results of Baert et al.[149] Again it seems that the treatment employed by Hirshfeld and Hope in 2-cyanoguanidine, by Eisenstein in cytosine monohydrate, and here by Baert et al., of a stockholder partitioning of the model electron density in the crystal in order to extract a molecular dipole moment is susceptible to large systematic errors and generally underestimates μ. The very high result of 62.7 obtained using Hirshfeld's multipole refinement strategy is somewhat disturbing, but Baert et al. have discussed this and attribute it to the larger number of often very diffuse monopole functions obtained in this refinement. The presence of diffuse electron density functions, of any type, in a refinement is contrary to a basic underlying principle of the rigid pseudoatom model; the individual pseudoatom electron distributions are assumed to "perfectly follow" the thermal motion of the nucleus at their origin. This has been framed by Kurki-Suonio[208] as the concept of "locality", and its adherence in a multipole refinement is not necessary but most desirable. The diffuseness of the pseudoatom model can usually be overcome by reducing the flexibility of the radial functions, in much the same manner as careful choice of basis sets in ab initio computations.

w. Barbital (**23**). Craven et al.[151] reported a value of 2.3 (40) for the dipole moment of **23** (5,5-diethylbarbituric acid) from a low-temperature combined X-ray and neutron study. This result is consistent with the value of 3.77 (3) reported in dioxane solution by Soundararajan.[197]

x. Benzenechromium tricarbonyl. Net atomic charges from a monopole refinement using low-temperature X-ray and neutron data[153] have been used with the neutron geometry reported in that work to derive a dipole moment of 18.3 (8.3). In spite of the relatively large error, this is in surprisingly good agreement with the measurement of 16.8 in benzene solution.[198]

y. Adenosine and Other Nucleosides and Nucleotides. In a pioneering study, Pearlman and Kim[111] collected low-temperature X-ray data on six different nucleotides and nucleosides in order to derive a complete set of experimental atomic charges for DNA. The data sets are extensive (with the exception of that for the guanosine 5′-monophosphate salt) but the resulting κ-refined atomic charges (and hence dipole moments) are necessarily compromised by the lack of neutron diffraction data. We have already discussed the dipole moments obtained for the water molecules in these studies, but unfortunately there are no solution measurements of μ for comparison with diffraction results for any of the nucleoside or nucleotide molecules. We note here that the dipole moments reported by Pearlman and Kim were obtained using the X-ray positions for the heavy atoms, and extending the lengths of the C–H, N–H, and O–H bonds to standard values. All molecules are neutral except for guanosine 5′-monophosphate which has a formal net charge of −2 (and for that reason we do not report its dipole moment in Table IV, although the original study tabulates a value with origin at the center of mass).

Klooster and Craven[155] have very recently reported multipole refinement results for adenosine, using both X-ray and neutron data at 123 K, and these provide a useful comparison with the monopole results obtained by Pearlman and Kim from X-ray data only. The dipole moment of 25.7 (17.0) reported by Klooster and Craven is considerably larger than that (8.0) obtained by Pearlman and Kim, even allowing for rather large experimental errors in both results. The source of this discrepancy has yet to be resolved.

2. The Enhancement of the Dipole Moment on Hydrogen Bonding

In discussing the diffraction estimates of μ we have repeatedly observed an enhancement of μ for molecules in strongly hydrogen bonded environments (e.g. water, urea, imidazole, cytosine, formamide, acetamide) and little change from solution values for molecules in crystals where such intermolecular interactions are weak or nonexistent (e.g. alloxan, *p*-nitropyridine *N*-oxide, benzenechromium tricarbonyl). The enhancement of molecular dipole moments upon hydrogen bonding is well established experimentally, especially for small hydrogen bonded dimers in molecular beams. Legon and Millen[209] have recently reviewed work on such dimers, and their Table VIII summarizes results for ten dimers; the enhancement of μ *for the dimer* (or sometimes the *a* component, μ_a) ranges from 0.14 D to 0.99 D (0.47 to 3.30 × 10^{-30} C m). Hermansson and Lunell[210,211] have noted the enhanced polarity (by 50–60%) of water molecules in ab initio studies of water in crystal fields appropriate to the crystal structures of $LiOH{\cdot}H_2O$ and $NaHC_2O_4{\cdot}H_2O$, and additional evidence that similar enhancements occur in crystals comes from the work of Cummins, Bacskay, and Hush[212,213] who studied by ab initio methods the change in the charge distributions of water and ammonia on going from gas phase to solid. Those workers mimicked the crystal environment by a set of point charges and used moments induced in a central molecule to define a new set of point charges; the process was iterated to self-consistency. In this manner Cummins et al. estimated dipole moment enhancements of 2.66 for water (in the ice Ih structure) and 1.70 for ammonia. Earlier simulation studies employing a polarizable model for water in ice Ih and the pure liquid[214] and water–amino acid interactions[215] yielded similar results.

The enhancement of the dipole moment of one molecule brought about by the proximity of another is of course a general effect, not restricted to hydrogen-bonded systems, and can be quantified using a perturbation theory approach based on a multipole expansion of the interaction Hamiltonian.[1,7] In this approach the dipole moment induced in one molecule by another depends on the electric field of one and the dipole polarizability of the other. Buckingham and coworkers[216,217] have used this approach, along with a partitioning of the multipole moments and polarizabilities of the monomers, to obtain near quantitative agreement with experiment for the dipole moments of several van der Waals dimers. For the present purposes a similar, but much simpler, approach can be used to gain some insight into induced dipole moments of urea molecules in the crystal. We choose urea here because it displays what appears to be a significant observable increase over the gas-phase value [between 5.2 (18) and 6.2 (18)], and because it has a particularly simple crystal structure.

The z component of the dipole moment induced by an electric field, $\mathbf{E}$, is given by

$$\mu_z^{\text{ind}} = \alpha_{zz}E_z \tag{29}$$

where α_{zz} is the component of the dipole polarizability tensor along z and E_z the z component of the field. The electric field resulting from a dipole, magnitude μ_z, directed along the positive z direction is given by

$$E_z = \frac{\mu_z}{4\pi\epsilon_0}\,\frac{3\cos^2\theta - 1}{r^3} \tag{30}$$

where θ is the normal azimuthal angle in spherical polar coordinates. Combining eqs 29 and 30 yields

$$\mu_z^{\text{ind}} = \frac{\alpha_{zz}\mu_z}{4\pi\epsilon_0}\,\frac{3\cos^2\theta - 1}{r^3} \tag{31}$$

For urea, which crystallizes in a tetragonal space group with all molecules (and hence dipole moments) directed either up or down the c axis, it is a simple matter to sum contributions to μ_z^{ind} over several adjoining unit cells; the electric field converges with the inclusion of only three unit cells surrounding a central cell. Using $\mu_z = 12.8 \times 10^{-30}$ C m (see Table II) and $\alpha_{zz} = 6.54 \times 10^{-40}$ C m^2 V^{-1} (a highly correlated value from Sanchez de Meras et al.;[218] no experimental value appears to have been reported), we obtain $\mu_z^{\text{ind}} = 2.57 \times 10^{-30}$ C m (0.77 D), in excellent agreement with the magnitudes observed for hydrogen-bonded dimers, and approximately one-half the enhancement implied by the diffraction results. This value is most likely an underestimate of μ_z^{ind} as it is only a first-order approximation; it neglects a self-consistent treatment (i.e. induced dipoles further alter the dipole moment), higher order terms in eq 29 such as hyperpolarizabilities, dipole–quadrupole and higher polarizabilities, and field gradient terms,[1] and is certainly not accurate for nearest neighbors.

This simple exercise could readily be repeated for other systems in Table IV. For example, we note that since the induced dipole depends upon the product $\alpha\mu$ we can estimate that imidazole [$\mu = 12.2 \times 10^{-30}$ C m (see Table IV) and $\alpha = 8.2 \times 10^{-40}$ C m^2 V^{-1} (from Calderbank et al.[186])] should display a similar, if not greater, enhancement, although much depends on the lattice sum to determine the electric field. It is not inconceivable that a molecule such as alloxan, which clearly has a substantial lattice energy, apparently as a result of close C=O···C intermolecular contacts in the crystal[164] may adopt a packing arrangement which exhibits a *negative* enhancement of μ, as suggested by the difference between the ab initio and diffraction results in Table IV. The simple estimation of induced dipole moments for molecular crystals, in the manner described above, would seem to be a worthwhile exercise.

We conclude this section by reiterating that the majority of diffraction estimates of μ exceed isolated molecule values, albeit by amounts of marginal significance at present. Nevertheless these enhancements appear to be of the correct order of magnitude and correlate with the dipole moment magnitude and polarizability of the molecules. Further experimental and theoretical model studies in this area are warranted.

3. The Direction of the Dipole Moment

The typically excellent agreement between diffraction estimates of μ and other experimental or theoretical results given in Table IV would seem to suggest that the gross molecular polarity is also well described and that the dipole moment direction is reliably retrieved from studies using diffraction data. This is indeed the case, as indicated by some of the preceding discussion of Table IV. In this section we hope to convincingly demonstrate that the direction of μ (i.e. all three components in general) is obtained to a high degree of accuracy, and we do this by concentrating on a small subset of molecules in Table IV: those where the direction is not defined by symmetry and where reliable independent information on μ is available from either the microwave Stark effect or ab initio theory.

There have been a very small number of such comparisons previously published: those on uracil,[12] formamide,[35,89,166,182] and 1-methyluracil[141] exhaust the literature. To update this important comparison, in Figure 1 we pictorially compare X-ray diffraction estimates of magnitude and direction of μ with microwave and ab initio results for formamide and uracil plus four other largely planar molecules. With the exception of uracil, the diffraction estimate of the dipole moment direction is within approximately 10° of any reliable independent estimate. The two monopole results for uracil are nearly 20° from the SCF/6-31G** vector (obtained at the 3-21G optimized geometry), but we note that the uracil data set was low resolution and room temperature, and the location of the hydrogen atoms was not aided by an independent neutron diffraction study. It is especially noteworthy that four separate determinations for formamide, multipole, monopole, DI-FB, and DI-DB (the latter is not included in the figure as it is indistinguishable from, but longer than, the DI-FB vector), deviate by at most 10° from the microwave gas-phase result. To put these deviations in perspective it is important to emphasize that the experimental error in the direction of μ is also typically 10° (e.g. 12° from Stewart[12] and 10° to 25° from Spackman et al.,[164] with the larger errors being associated with less precise and lower resolution high-temperature data). The comparison of dipole moment directions for 1-methyluracil by Klooster et al.[141] demonstrates that their refinements II and IIv (which used the same X-ray data set and neutron position and thermal parameters at the same temperature) yield dipole moments with directions close to those obtained for uracil, while the result of their refinement I (which used an X-ray data set at a significantly different temperature) is considerably different. As discussed

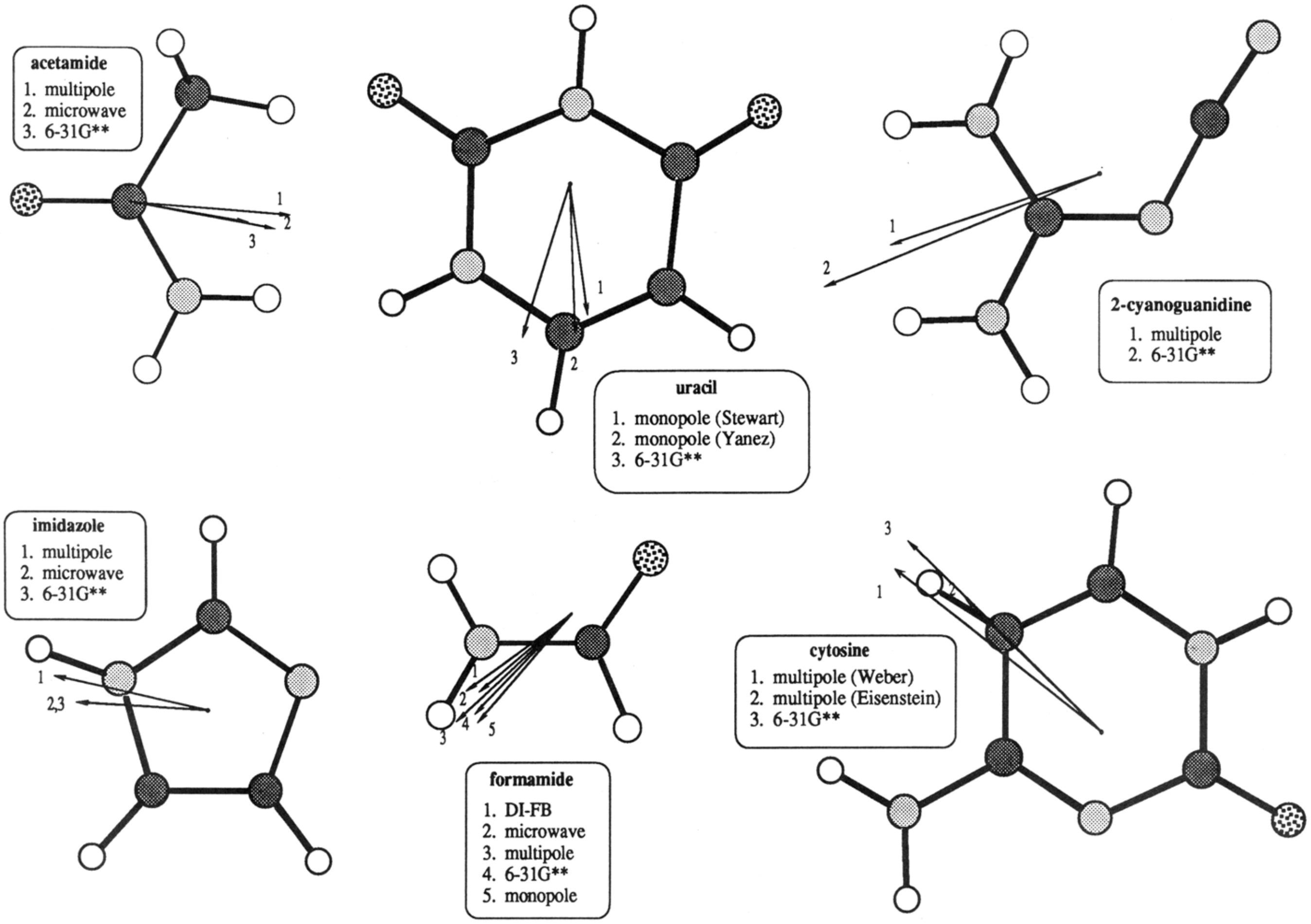

Figure 1. Comparison of diffraction estimates of dipole moment directions with microwave and ab initio 6-31G** results.

above there were significant problems encountered in that refinement.[141]

It is tempting to attribute the deviation of the dipole moment direction from that observed in the gas phase to intermolecular interactions, but such conclusions would be premature. There are only three microwave results reported in Figure 1, and of those only that for imidazole could be considered worthy of more detailed study as it is the only one for which neutron diffraction results were used to unambiguously determine hydrogen atom positions and thermal motion parameters. Nevertheless, this aspect of the determination of electric moments from diffraction data would seem to be worthy of future study.

B. Quadrupole and Second Moments

Discussion of diffraction estimates of quadrupole or second moments is somewhat more difficult than that for dipole moments. As mentioned earlier the quadrupole moment tensor has, in general, six unique components, referred to a specific coordinate system and associated origin. Here we discuss in some detail diffraction estimates of both quadrupole and second moments for 13 molecules where diffraction results have either been reported in the literature, or can be inferred from literature data. All results are given with respect to the center of mass, but the choice of coordinate axes is rather more problematic in some instances. We make the following choices:

(i) For linear molecules (chlorine and acetylene) or molecules with a 3-fold or higher rotation axis (benzene and *s*-triazine) z is the major axis; Θ_{zz} is unique.

(ii) For molecules of D_{2h} or C_{2v} symmetry (water, urea, ethylene, pyrazine, and *p*-dicyanotetrafluorobenzene) the major symmetry axis is z, and the molecule is assumed to lie in the xz plane; any two diagonal components of Θ are unique.

(iii) For planar asymmetric molecules (formamide, 2-cyanoguanidine, imidazole, and cytosine) we report Θ with respect to the principal inertial axes; any two diagonal components of Θ plus one off-diagonal component are unique (with this choice of coordinate system comparisons with experimental values obtained via the molecular Zeeman effect are more straightforward, although by no means easy as we demonstrate below).

The choice of axes for the planar asymmetric molecules is given in Figure 2, and Table V summarizes diffraction estimates of quadrupole moments for all 13 molecules, and compares them with available experimental and theoretical results. As for the dipole moment above, we discuss each of the systems in Table V in turn; numerical results will be assumed to be in SI units in all discussion (i.e. must be multiplied by 10^{-40} C m^2).

1. Discussion of Quadrupole Moment Results

a. Chlorine. The collection of single-crystal X-ray diffraction data on molecular chlorine at 90 K by Stevens[104] was an exceptional piece of work. Stevens performed three different multipole refinements including up to hexadecapole functions, and the electron density parameters resulting from these are reported

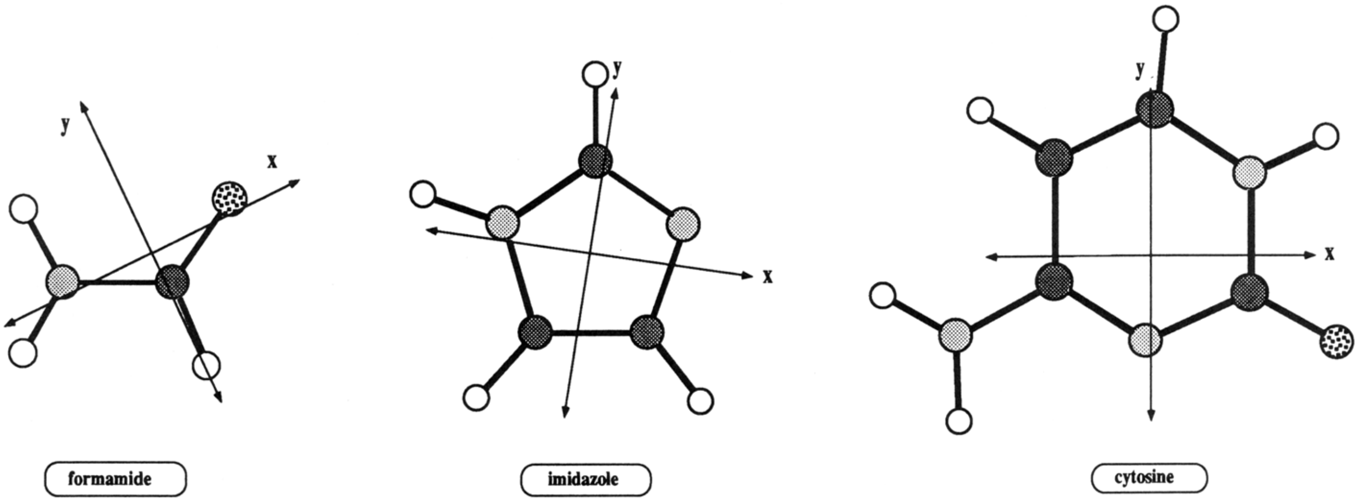

formamide imidazole cytosine

Figure 2. Principal in-plane inertial axes for planar asymmetric molecules.

Table V. Diffraction Estimates of Quadrupole Moments Compared with Other Experimental Results, Where Available, and with ab Initio Theory

molecule	diffraction results			other experiment or theory
Cl_2	Θ_{zz}	+11.0 (20)	multipole[104]	+10.8 (5)/gas[54]
chlorine		+7.7 (20)	multipole[104]	+16.5 (17)/gas[219]
				+8.91/6-31G**
H_2O	Θ_{xx}	+11.0	multipole[105]	+8.77 (7)/gas[63]
water		+3.3	multipole[106]	+7.93/6-31G**
	Θ_{yy}	−13.0	multipole	−8.34 (7)/gas
		−2.9	multipole	−7.59/6-31G**
	Θ_{zz}	+2.0	multipole	−0.43 (10)/gas
		−0.4	multipole	−0.33/6-31G**
CH_3NO	Θ_{xx}	−0.6 (26)	monopole[114]	−1.0 (7)/gas[220]
formamide (**4**)				−4.44/6-31G**
	Θ_{yy}	+9.1 (18)	monopole	+11.3 (13)/gas
				+12.58/6-31G**
	Θ_{zz}	−8.5 (14)	monopole	−10.3 (27)/gas
				−8.14/6-31G**
	Θ_{xy}	−5.5 (12)		−4.87/6-31G**
CH_4N_2O	Θ_{xx}	+38.7 (60)	multipole[115]	+30.03/6-31G**
urea (**5**)		+36.4 (60)	multipole[115]	
	Θ_{yy}	−35.4 (40)	multipole	−19.00/6-31G**
		−30.0 (40)	multipole	
	Θ_{zz}	−3.3 (43)	multipole	−11.04/6-31G**
		−6.3 (40)	multipole	
C_2H_2	Θ_{zz}	+24.3 (58)	multipole[118]	+20.1 (6)/gas[221]
acetylene		+19.0 (36)	multipole[118]	+23.23/6-31G**
		+25.9 (38)	monopole[118]	
		+21.3 (53)	monopole[118]	
		+20.3	DI-FB[35]	
C_2H_4	Θ_{xx}	+5.7	multipole[118]	+4.7/gas[222]
ethylene				+5.4 (3)/gas[223]
				+4.99/6-31G**
	Θ_{yy}	−7.8	multipole	−12.0/gas
				−10.8 (7)/gas
				−11.04/6-31G**
	Θ_{zz}	+2.1	multipole	+7.3 (10)/gas
				+5.4 (3)/gas
				+6.05/6-31G**
$C_2H_4N_4$	Θ_{11}	+16.2	multipole[120]	+27.23/6-31G**
2-cyano-		+27.2	multipole[120]	
guanidine (**6**)	Θ_{22}	+0.3	multipole	−12.95/6-31G**
		−4.0	multipole	
	Θ_{33}	−16.5	multipole	−14.28/6-31G**
		−23.2	multipole	
$C_3H_3N_3$	Θ_{zz}	−20 (13)	multipole[224]	−2.8 (31)/solution[225]
s-triazine (**11**)		−24 (16)	multipole[224]	+2.03/6-31G**
		−2.7 (12)	monopole[224]	
		−3.5 (6)	monopole[224]	
		−1.2 (4)	monopole[12]	
$C_3H_4N_2$	Θ_{xx}	+19.4	multipole[129]	−3.1 (9)/gas[226]
imidazole (**12**)				−1.58/6-31G**
	Θ_{yy}	+3.3	multipole	+22.6 (11)/gas
				+17.43/6-31G**
	Θ_{zz}	=22.7	multipole	−19.6 (18)/gas
				−15.84/6-31G**
	Θ_{xy}	−19.4	multipole	−9.61/6-31G**
$C_4H_4N_2$	Θ_{xx}	+37.5	multipole[35]	+40.47/6-31G**
pyrazine (**15**)	Θ_{yy}	−9.8	multipole	−8.83/6-31G**
	Θ_{zz}	−27.7	multipole	−31.64/6-31G**
	Θ_{xx}	+55.0	multipole[134]	+8.56/6-31G**
$C_4H_5N_3O$	Θ_{yy}	+6.8	multipole	+8.56/6-31G**
cytosine (**17**)	Θ_{zz}	−61.8	multipole	−17.11/6-31G**
	Θ_{xy}	+66.2	multipole	+45.4/6-31G**
	Θ_{zz}	−40.3 (35)	multipole[227]	−29.0 (17)/gas[228]
		−32.3 (35)	multipole	−28.3 (12)/solution[57]
C_6H_6		−28.7 (35)	monopole	−28.30/6-31G**
benzene	Θ_{xx}	−4.7 (50)	multipole[229]	+34.61/6-31G**
		−6.9	multipole	
$C_8N_2F_4$	Θ_{yy}	+72.5 (46)	multipole	+72.61/6-31G**
p-dicyanotetra-		+61.5	multipole	
fluorobenzene	Θ_{zz}	−67.8 (88)	multipole	−107.22/6-31G**
		−54.6	multipole	

[a] All quantities in SI units (i.e. $\Theta/10^{-40}$ C m^2; see Table I for conversion factors). Other experimental results are labeled as either "gas" (i.e. microwave Zeeman or induced birefringence), or "solution" (induced birefringence in a nonpolar solvent); see text for details. 6-31G** ab initio results have been obtained at the SCF level, generally at the neutron crystal geometry.

in his Table 5. The refinement labeled D included only harmonic thermal motion parameters and imposed cylindrical symmetry on the molecule (the molecule possesses only a crystallographic inversion center); that labeled E was as for D but with additional third- and fourth-order anharmonic thermal parameters; F was as for E with the constraint on cylindrical symmetry relaxed. We have used the multipole parameters from Stevens to compute the Θ_{zz} values reported in Table V.[230] The results of +11.0 (20) from refinement D and +7.7 (20) from both E and F are in very good agreement with the gas-phase electric field gradient induced birefringence result [10.8 (5)] of Buckingham, Graham, and Williams,[54] but are significantly lower than the value of 16.5 (17) reported earlier by Emrich and Steele.[219] The concordance between induced birefringence and diffraction estimates of Θ_{zz} for chlorine is most impressive; not only is the magnitude of Θ_{zz} retrieved from the X-ray diffraction data, but most importantly the sign is also correct; we note with interest that the X-ray study predates both induced birefringence studies.

b. Water. The water molecules in cytosine monohydrate do not possess ideal C_{2v} symmetry; the three components reported in Table V have been obtained by diagonalization of the second moment tensor in each case (the principal directions are indeed close to the inertial axes of the molecule). Because of this procedure it is difficult to report precise estimates of errors, but we can say that the error obtained in each second moment component from the data of Weber and Craven[105] was as much as 6 or 7 × 10^{-40} C m^2 (see section V.B.2), which suggests errors of nearly 50% may be assigned to the larger values in Table V. Eisenstein did not report error estimates and, as observed for the dipole moment, her quadrupole moment results display systematic differences from those of Weber and Craven. Again, those obtained by construction of a pseudomolecule by summation of pseudoatom fragments are in better accord with the gas-phase results.[63] The comparison of diffraction estimates of Θ for water, obtained in a crystalline hydrate, with gas-phase values obtained in molecular beams, can hardly be expected to be fruitful however, as numerous studies have demonstrated the radical changes in the electron distribution of the water molecule upon participation in hydrogen bonding.

c. Formamide (4). Moss[169] has reported pseudoatomic second moments for formamide by direct integration of the X-ray diffraction data of Stevens.[114] Unfortunately Moss reported only the diagonal components (in a different coordinate system for each atom), which preclude any rotation and summation to obtain molecular moments. Instead, we have used point charges obtained by Stevens from a κ-refinement using the X-ray data (see his Table 7) and the molecular structure obtained by Stevens in a high-order refinement with the same data, to estimate components of the quadrupole moment tensor with respect to the principal inertial axes (in this case of the X-ray structure—see Figure 2). The diagonal components agree very well with those obtained by Tigelaar and Flygare[220] from the molecular Zeeman effect, and the experimental errors quoted in the two experiments are of a similar magnitude. It is well worth emphasizing that the molecular Zeeman effect cannot yield off-diagonal components of Θ (unless isotopic substitution experiments are performed), but the diffraction experiment can, and the estimate of $\Theta_{xy} = -5.5$ (12) so obtained is in accord with the SCF/6-31G** value of −4.87.

d. Urea (5). The model electron distribution parameters obtained by Swaminathan et al.[115] have been used to compute the two sets of values reported in Table V; as discussed above the two multipole refinements differed only in the radial exponents chosen, and hence should yield similar results. This is indeed the case, and the diffraction results for the two in-plane components (Θ_{xx} and Θ_{zz}) agree with the 6-31G** results, but the diffraction estimates of the out-of-plane component are almost twice the ab initio value. As for the dipole moment, we note that urea is very strongly hydrogen bonded in the crystal; the extent to which this is reflected in the quadrupole moment tensor is unknown at present. In the section following we discuss second moment (rather than quadrupole moment) results for urea and other molecules to gain some insight into whether these discrepancies are indeed significant.

e. Acetylene. The saga of quadrupole moment determinations from diffraction data for acetylene is lengthy and replete with wrong turns, but worthy of detailed examination. The single-crystal X-ray diffraction data on the cubic phase of acetylene, collected by van Nes and van Bolhuis[118] at 141 K, was limited to a sphere of 0.80 Å^{-1} by the large librational motion of the molecules. Nevertheless the data were accurate and extensive enough to enable a restricted multipole analysis to be performed; in the absence of neutron data spectroscopic information was used to constrain the proton positions and motion. Those authors performed two monopole refinements (A1 and A2 in their Table 5) and two multipole refinements (A3 and A4) containing deformation functions up to the quadrupole level. Van Nes and van Bolhuis actually reported Θ_{zz} values of 33 and 26 from refinements A3 and A4 and compared them with a value of 10 apparently given by Gordy, Smith, and Trambarulo.[231] Gordy et al. in fact report a value of 5.3 × 10^{-26} esu from microwave line broadening; this is far from a definitive result as it is *unsigned* and refers to a quadrupole moment operator defined as twice the normal convention (i.e. twice that in eq 7). Van Nes and van Bolhuis took this poor agreement with the free molecule value to be discouraging and concluded that data of the quality of that collected for acetylene were not very suitable for this type of work unless a companion neutron study was performed. That may be a sensible conclusion, but it is not entirely justified by the comparison of Θ_{zz} values.

We have recomputed Θ_{zz} from the multipole parameters reported by van Nes and van Bolhuis, obtaining +24.3 (58) and +19.0 (36) for refinements A3 and A4, respectively, and these are the values given in Table V. We have also computed quadrupole moments from the point charges obtained in the two monopole refinements: the results of +25.9 (38) and +21.3 (53) for refinements A1 and A2 agree well with the multipole refinement values. Quite independently, Moss[169] performed a direct integration of the diffraction data to obtain a value of +1.27 e Å^2 (or +20.3 in SI units). Unfortunately Moss converted the values reported by van Nes and van Bolhuis (originally in SI units) to e Å^2 incorrectly to obtain an unfavorable impression of his DI-FB result. Other experimental determinations of Θ_{zz} for acetylene have yielded values in the range 11 to +28. The other experimental result we list in Table V is from a very recent temperature-dependent study by Coonan and Ritchie[221] of the Cotton–Mouton effect in the gas phase, in conjunction with the polarizability anisotropy and molecular *g* value from a separate experiment; their result of +20.1 (6) is probably the most reliable experimental value, and is in accord with the MRSDCI-ANO ab initio result (including vibrational corrections) of +19.2 (5) reported recently in a definitive study by Lindh and Liu.[232]

The agreement between the different diffraction estimates of Θ_{zz} is remarkable: they span a range from +19.0 to +25.9 with a typical (and large) experimental error of ~4.0. Moreover they are all in accord with the best experimental and theoretical values. It is clear that no matter what strategy is employed to extract Θ_{zz} from the diffraction data, the correct sign and magnitude of this property are emphatically contained in the X-ray data, even at the simple point charge level of representing the charge distribution.

f. Ethylene. The 85 K X-ray data of van Nes and Vos[119] is more extensive than that obtained for acetylene, but as for acetylene the electron density study suffers from the effects of large amplitudes of thermal motion and the lack of neutron data to unambiguously assign position and thermal parameters. Van Nes and Vos reported the results of two multipole refinements (A and B in their Table 6), and we have used the parameters from the best fitting model (A) to compute components of Θ. The results are in satisfactory agreement with gas-phase values of Kukolich et al.[222] and Dagg et al.[223] which are actually in significant disagreement with each other. Both gas-phase results are in essential agreement with the 6-31G** values, but neither should be considered definitive as one has been inferred from the ethylene–hydrochloride complex, and the other from collision induced absorption.

g. 2-Cyanoguanidine (**6**). Hirshfeld and Hope[120] reported quadrupole moments for **6** derived from their multipole refinements using both strategies discussed above in the retrieval of dipole moments. Unfortunately, the quadrupole moments given were *principal values* (i.e. Θ has been diagonalized), but Hirshfeld and Hope neglected to report the corresponding principal directions (except that Θ_{22} is perpendicular to the molecular plane). The smaller diffraction estimates in Table V (upper entry in each case) are from a sum of pseudoatom fragments, and the larger values from a stockholder partitioning of the model electron density in the crystal. As observed for the dipole moment, the latter yields results which differ systematically from the usual summing of pseudoatom moments, although the situation is less clear here because the conversion to traceless quadrupole moments necessarily mixes all second moments. It is difficult to decide which diffraction result is in better agreement with the 6-31G** (principal) values reported in the table, and the comparison is even more clouded by the fact that all three results refer to slightly different sets of axes in the molecular plane.

h. s-Triazine (**11**). This molecule was the subject of a pioneering study by Coppens[127] who reported deformation electron density maps from a combination of X-ray and neutron diffraction data at room temperature. Price, Maslen, and Delaney[224] subsequently performed monopole and multipole refinements using Coppens' X-ray data, and we have used their results to compute the quadrupole moment (the molecule has crystallographic D_{3h} symmetry so there is only a single unit component, Θ_{zz}). From Table V we see that the multipole refinements yield quadrupole moments which are large and negative, albeit with quite large errors of nearly 70%. The monopole refinements from Price et al. (i.e. point charge models) on the other hand suggest that Θ_{zz} is very small and negative, although still with a large experimental error, and the value of −1.2 (4) inferred by the set of point charges reported by Stewart[12] from an *L*-shell refinement of the same X-ray data is in agreement with this conclusion. For comparison we have listed the recent value obtained by Dennis from observation of the electric field gradient induced birefringence in cyclohexane solution. No other experimental values are known to us, but the ab initio 6-31G** result of +2.03 seems to support the solution value from Dennis and the monopole refinement results and casts doubt on the large negative results derived from multipole refinements. What could be the origin of this rather large discrepancy? To explore this further we have performed independent multipole refinements (up to the quadrupole level on each center) using Coppens' X-ray data; the resulting model deformation electron density maps displayed significant sharp quadrupolar features near the C and N nuclei, features which are clearly unrealistic based upon maps obtained for similar compounds and which would necessarily compromise the extraction of quadrupolar deformation functions on the heavy atoms (and hence the molecular quadrupole moment). A monopole refinement would not suffer from the same problems, and it would appear that all such models obtained in fitting the present X-ray data yield results for Θ_{zz} which are consistent with the induced birefringence result. Finally we note that in a study of the lattice energy of *s*-triazine, Mason and Rae[233] found that a quadrupole moment of ±9.3 provided a minimum lattice energy at the experimentally observed *c*-axis length. It would be worthwhile collecting new X-ray and neutron diffraction data on *s*-triazine at lower temperature to clarify the situation with the present quadrupole moment determinations.

i. Imidazole (**12**). The results in Table V have been calculated from the multipole refinement reported by Epstein et al.[129] and refer to the inertial axes of the molecule at the gas-phase microwave geometry[185] (see Figure 2). No experimental errors are given for the diffraction estimates because of the diagonalization and rotation that has been performed, but we can safely assume that the error in each component is likely to be of the order of 3.0, since that is the average error computed in individual components of the second and quadrupole moment tensors in the crystal coordinate system (see section V.B.2). With the exception of Θ_{zz}, the out-of-plane component, agreement with the gas-phase molecular Zeeman results of Stolze and Sutter[226] is extremely poor, and it is initially tempting to assert that the two experimental results refer to coordinate systems with x and y axes interchanged. Such is not the case however, as the 6-31G** results reported in the table have been obtained using the neutron diffraction geometry in the crystal, with Θ diagonalized and rotated into the same coordinate system as the two experimental sets of results in the table (i.e. inertial axes for the gas-phase microwave geometry). 6-31G** results computed at the gas-phase geometry are $\Theta_{xx} = -3.25$, $\Theta_{yy} = +24.15$, $\Theta_{zz} = -20.90$, and $\Theta_{xy} = +11.32$, the diagonal components of which are in excellent agreement with Stolze and Sutter's values. Clearly the different geometry in the crystal is responsible for a small part of the discrepancy observed between the two sets of experimental results, and we explore the remaining differences in more detail below in our discussion of second moments.

j. Pyrazine (**15**). Moss and Feil[35] performed careful multipole refinements of the low-temperature X-ray data of de With and Feil,[132] exploring in detail the quality of the fit as a function of the refined C–H bond length, which in turn depended critically upon the exponent of the radial functions on the hydrogen atoms.

This study of dependence upon C–H distance was necessitated by the lack of complementary neutron data. Moss and Feil reported quadrupole moments computed from six different multipole models, with r_{CH} ranging from 0.967 to 1.203 Å. The values reported in Table V are from the model which yields r_{CH} = 1.076 Å, in good agreement with independent estimates of this structural parameter. Clearly these diffraction estimates are in excellent agreement with the 6-31G** results tabulated, and also with the recent CI results obtained with a TZVP basis set, reported by Walker and Palmer[234] ($\Theta_{xx} = +39.96$, $\Theta_{yy} = -6.64$, $\Theta_{zz} = -33.32$). Moss and Feil did not discuss or report errors in their derived quadrupole moments, but they are likely to be considerable. We can estimate a systematic error from the dependence of their results on C–H distance: in this manner we estimate shifts of +5.1, −4.3, and −0.8 (for Θ_{xx}, Θ_{yy}, and Θ_{zz} respectively) for a small increase of 0.03 Å in the assumed C–H distance, which would suggest conservative error estimates of at least 3.0 in each component, similar to error estimates in similar studies of diffraction data. Considering these large errors and the deficiencies of the present diffraction data, it would seem a profitable exercise to collect and analyze combined low-temperature X-ray and neutron diffraction data in order to better determine the quadrupole moment tensor for this simple highly symmetric molecule; there are no other experimental estimates of Θ at present.

In a separate important study, Moss and Feil have also calibrated the multipole refinement strategy for extracting molecular quadrupole moments from diffraction data in their analysis of a model set of diffraction data for pyrazine.[235] Those authors constructed an idealized set of structure factors from Fourier transforms of the molecular wave function reported by Almlof et al.[236] and analyzed it in the manner pursued in their earlier experimental study.[35] Their most flexible multipole model yielded components (Θ_{xx}, Θ_{yy}, Θ_{zz}) = (45.5, −8.9, −37.5), which are in good agreement with the values of (+46.6, −6.6, −40.0) obtained directly from that particular molecular wave function. The success of a model study such as this lends significant support to the proposition that molecular electric moments can be reliably determined from diffraction data, although this particular study yielded results that would appear to be at variance with those obtained by Moss and Coppens[170] in their similar model study of the dipole moment in formamide. Again it would appear that more model studies are called for.

k. Cytosine (*17*). As for imidazole, we report components of Θ with respect to the inertial axes (in this case for the neutron geometry) of the molecule (see Figure 2), and as observed for imidazole the agreement with ab initio 6-31G** values is poor, with the possible exception of the off-diagonal in-plane component, Θ_{xy}. We explore these large discrepancies below in our analysis of second moments.

l. Benzene. The combined X-ray and neutron data collected on deuterated benzene at 123 K have been analyzed by Jeffrey and co-workers,[144,145] although the electron density analysis appears not to have been published. We have independently performed monopole (κ) and multipole refinements using the 123 K X-ray data with fixed position parameters from the neutron study. The two multipole refinements differed only in their use of neutron thermal parameters for all atoms (upper entry in Table V) or fixed neutron thermal parameters for H atoms with those for C atoms allowed to be determined by the X-ray data (lower entry). The quadrupole moment tensors computed from these parameters have been diagonalized (the molecule possesses only an inversion center in the crystal) and the out-of-plane component reported as Θ_{zz} in Table V. In all refinements the two in-plane components are equal within the estimated experimental errors. The diffraction estimates obtained from the monopole refinement and the multipole refinement with fixed neutron thermal parameters for all atoms agree well with the electric field gradient induced birefringence measurements of Battaglia et al.[228] in the gas phase, and the value obtained in carbon tetrachloride solution by Dennis et al.[57] As observed for acetylene, the point charges obtained from the κ-refinement procedure, which imply a charge transfer of 0.15 (2) electrons from H to C, provide an excellent estimate of Θ_{zz}. However, allowing thermal parameters on the C atoms to vary in the multipole refinement yields an estimate for Θ_{zz} which appears to be too large. This dependence on the thermal parameters is not surprising; both local quadrupolar deformations of the electron density and harmonic thermal parameters have the same symmetry and will always be correlated to some extent. We discuss this in more depth in the following section.

m. p-Dicyanotetrafluorobenzene. The absence of hydrogen atoms in this molecule would appear to obviate the need for neutron diffraction data, hence the extensive 98 K X-ray data from Dunitz et al.[148] should provide an excellent opportunity to critically examine the extraction of quadrupole moments from diffraction data. Hirshfeld[93,229] has analyzed the data with a multipole refinement model and reported atomic and molecular second moments from both a pseudomolecule (i.e. sum of pseudoatom fragments) with associated error estimates and from a stockholder partitioning of the model density in the crystal. In reanalyzing these figures we have discovered that there appears to be an error in the computation of the molecular second moments from the atomic values for the two in-plane components; Hirshfeld seems to have omitted the factor of 2 in the expression

$$\mu_{zz}^{\mathrm{mol}} = \sum_{a} [z_a^{\,2} q_a + 2 z_a \mu_{a,z} + \mu_{a,zz}]$$

The values reported in Table V have been obtained from second moments computed with the correct expression. The upper entry in the table refers to a pseudomolecule sum of fragments and the lower figure to the stockholder-partitioned result. In this case both strategies yield similar values, especially when the experimental errors in the pseudomolecule approach are taken into account, yet neither set of diffraction estimates is in particularly good agreement with the results of a 6-31G** calculation, nor do they agree with the rather similar results obtained in a local density functional calculation by Delley ($\Theta_{xx} = +39.9$, $\Theta_{yy} = +63.5$, $\Theta_{zz} = -103.5$).[237]

2. Second Moments vs Quadrupole Moments

In the foregoing discussion we have repeatedly observed that for many molecules, particularly those of lowest symmetry, the comparison between diffraction estimates of components of Θ and other experimental or theoretical values is obscured by the mixing of second moment terms to form the appropriate quadrupole moment expression. The traceless quadrupole moment tensor is a very sensitive measure of the anisotropy of the molecular charge distribution; what we wish to establish in this section is whether the reliability of the diffraction estimate of this quantity is irretrievably compromised by the experimental errors in the various second moments, or whether in fact the large discrepancies between diffraction estimates and other results observed for systems such as imidazole and cytosine are a consequence of strong intermolecular interactions in the crystal, or perhaps an artifact of the refinement procedure. To do this we examine the second moments obtained from the diffraction experiment for a subset of the molecules discussed above. However, before engaging in a detailed discussion it is worthwhile outlining the differences between second and quadrupole moments and the manner in which they are presently obtained from diffraction data, typically from a multipole refinement.

In section IV.B we outlined the multipole refinement procedure, and eqs 24 and 25 exemplify the summation of pseudoatomic charges and dipole and quadrupole moments to obtain molecular moments. The pseudoatomic moments are usually, but not always, obtained from a multipole refinement performed with respect to a single Cartesian coordinate system defined with respect to the unit cell axes in the crystal, and the computation of these atomic moments and their associated errors, as well as their contraction to molecular values, is performed in this coordinate system. However, this frame is seldom the most convenient for reporting the results or for comparison with other values, hence various rotations (such as a diagonalization) are usually performed, which generally hinders the reporting of precise error estimates in the resulting quantities. In this section we wish to compare diffraction estimates with ab initio theory as closely as possible, and it is essential to incorporate reliable experimental errors into the discussion. To this end we report "raw" second-moment values, those which have been obtained directly from the multipole refinement in the coordinate system chosen for the least-squares process. The experimental errors reported are obtained from $\sigma(c_{lm\pm})$, which derive from the diagonal elements of the inverse least-squares matrix; off-diagonal terms (i.e. correlation coefficients) have not been taken into account. Although strictly speaking we should incorporate them into the computation, and it is not in principle difficult to do so, propagation of errors using only the variances should yield meaningful errors in diffraction estimates of $\mu_{\alpha\beta}$, and these will suffice for the present.

A subtle difference between the quadrupole and second moments arises from the manner in which these quantities are extracted from the electron distribution in the crystal. As given by eq 21 the pseudoatom electron density is generally expressed as a sum of a spherical atom electron density, $\rho_{at}(r)$, and a term representing the asphericity (deformation) of the pseudoatom:

$$\sum_{l}^{L}\sum_{m=0}^{l} c_{lm\pm}R_l(r)y_{lm\pm}(\theta,\phi)$$

The traceless nature of the quadrupole moment tensor means that we can ignore the spherical atomic terms in the calculation, since the quadrupole moment of a neutral, spherically symmetric charge distribution (and hence of a collection of such distributions, the promolecule) is precisely zero. This is not the case for the second moments, and almost all second moments reported in the charge density literature have been obtained by numerical integration of the *deformation density*, $\Delta\rho$. For comparison with other values, we need to add to these values the contribution arising from the promolecule. Fortunately this term can be readily calculated; since the spherical atom charge distributions are neutral (i.e. they include the nuclear charge) then from eq 10 their second moments are origin independent. Moreover, since the function is spherical, then $\langle x^2\rangle = \langle y^2\rangle = \langle z^2\rangle = {}^1/_3\langle r^2\rangle$, and $\langle xy\rangle = \langle xz\rangle = \langle yz\rangle = 0$. The spherical atomic electron densities usually used in charge density work are the analytical Hartree–Fock limit functions from Clementi[238] or the more recent compilation by Clementi and Roetti.[239] Computation of $\langle r^2\rangle$ using these functions is straightforward and the results have been tabulated, along with other radial expectation values, by Boyd.[240] Using these quantities we can readily obtain second moments of the total molecular electron distribution; e.g. for μ_{xx}

$$\mu_{xx}(\rho_{tot}) = \mu_{xx}(\Delta\rho) + {}^1/_3 \sum_{\text{atoms a}} \langle r^2\rangle_{\text{spherical atom}} \quad (32)$$

We have used this strategy to obtain the second moments for 2-cyanoguanidine and *p*-dicyanotetrafluorobenzene reported in Table VI. For the other molecules, for which we have obtained quadrupole moments in Table V from a summation of point charges, dipoles and quadrupoles, we must incorporate the expectation values $\langle x^2\rangle = \langle y^2\rangle = \langle z^2\rangle = {}^1/_3\langle r^2\rangle$ for each of the monopole electron density functions: e.g. for μ_{xx}

$$\mu_{xx}(\rho_{tot}) = \mu_{xx}(\text{point moments}) + {}^1/_3 \sum_{\text{atoms a}} \langle r^2\rangle_{\text{pseudoatom}} \quad (33)$$

These expectation values are readily calculated and the resulting second moments for several molecules are included in Table VI.

The results for water derive from cytosine monohydrate.[105] Nevertheless, there is good agreement with 6-31G** values for all components and even for the off-diagonal terms which have large experimental errors. There are, however, differences of marginal significance. For example μ_{xx} and μ_{zz} are both smaller than theory predicts, and as a consequence the diffraction estimate for $\langle r^2\rangle$ is less than the ab initio value, but only just outside the estimated experimental errors.

The diffraction estimates of $\mu_{\alpha\beta}$ for urea display similar trends, with both in-plane components (μ_{xx} and μ_{zz}) significantly less than theory for both multipole refinements. In contrast, the out-of-plane component, μ_{yy}, is in excellent agreement with theory in both instances. As for water $\langle r^2\rangle$ is smaller than the ab initio value, but now by quite significant amounts [30.1 (83) and 23.4 (66) for the two refinements]. These lower estimates of μ_{xx} and μ_{zz} are the source of the poor

Table VI. Diffraction Estimates of Second Moments Compared with ab Initio 6-31G Results Obtained at the Same Geometry and with Respect to the Same Coordinate System**[a]

molecule	method	μ_{xx}	μ_{yy}	μ_{zz}	μ_{xy}	μ_{xz}	μ_{yz}
water[b]	multipole	−15.4 (24)	−21.4 (23)	−14.6 (41)	−0.4 (15)	−2.5 (16)	−6.7 (15)
	6-31G**	−18.93	−20.67	−17.13	+0.35	−1.09	−4.75
urea[c]	multipole	−64.6 (37)	−86.1 (24)	−36.7 (70)			
	multipole	−68.9 (29)	−84.7 (24)	−40.5 (54)			
	6-31G**	−79.87	−85.17	−52.49			
2-cyanoguanidine[d]	multipole	−95.3	−116.2	−129.0			
	multipole	−104.9	−115.5	−126.7			
	6-31G**	−96.45	−123.2	−124.2			
imidazole[b]	multipole	−100.8 (33)	−95.8 (44)	−67.5 (60)	+0.3 (23)	−10.3 (21)	+13.7 (27)
	6-31G**	−101.45	−85.06	−89.96	+5.46	−1.40	+13.97
cytosine[b]	multipole	−129.7 (109)	−60.1 (141)	−149.8 (71)	+28.6 (86)	−9.4 (46)	−18.7 (51)
	6-31G**	−173.94	−100.45	−160.75	+16.33	+2.38	−5.25
benzene[b]	multipole	−126.4 (34)	−111.0 (51)	−126.5 (39)	−7.5 (23)	−19.2 (25)	−6.2 (23)
	multipole	−116.2 (27)	−105.7 (41)	−116.0 (32)	−6.8 (18)	−15.6 (20)	−5.1 (18)
	6-31G**	−117.72	−106.70	−117.87	−4.85	−13.34	−4.94
p-dicyanotetrafluorobenzene[e]	multipole	−329.7 (87)	−287.6 (24)	−236.2 (8)			
	multipole	−315.8	−284.0	−238.4			
	6-31G**	−359.50	−264.95	−239.62			

[a] Choice of x and y axes is indicated in terms of the crystallographic axes; in all cases z completes a right-handed set of Cartesian axes. All quantities in SI units (i.e. $\mu_{ij}/10^{-40}$ C m^2; see Table I for conversion factors). [b] $x \| a, y \| b^*$. [c] x along 2-fold axis, z in molecular plane. [d] Principal directions; x and z in molecular plane. [e] x along 2-fold axis, y in molecular plane.

agreement of quadrupole moment components in Table V, but the analysis in terms of second moments is somewhat more illuminating.

For 2-cyanoguanidine two multipole results are reported as in Table V; the upper is from a summation of pseudoatom moments and the lower entry from a stockholder partitioning of the model electron density in the crystal. Unfortunately the comparison with theory here is obscured by the fact that Hirshfeld and Hope[120] reported only principal components in each case (hence we report principal components of the ab initio 6-31G** tensor in Table VI) and gave no estimates of experimental errors. In the absence of this information it is impossible to critically compare experiment with theory.

As observed above, imidazole and cytosine are strongly hydrogen bonded in the crystal, and diffraction estimates of their quadrupole moment tensors are in poor agreement with theory. In Table VI we clearly see that the source of those discrepancies is the systematic underestimate of one or more second moment terms by large and significant amounts. For imidazole we see that μ_{zz} is smaller than theory by 22.5 (60), and for cytosine μ_{xx} is smaller by 44.2 (109) and μ_{yy} by 40.4 (141). In terms of $\langle r^2 \rangle$, this quantity is underestimated by 12.4 (81) for imidazole and by 95.5 (192) for cytosine (a decrease by more than 20% in the latter case). It is important to note that although these differences, as well as those observed for water and urea, are all barely significant, it is the *systematic* nature of these which is probably most significant, and which is undoubtedly deserving of closer scrutiny. This reduction in diagonal components of the second moment tensor is also in accord with results obtained in terms of local atomic moments in model studies of hydrogen bonding in oxalic acid dihydrate.[241]

Benzene, on the other hand, is not hydrogen bonded in the crystal, and we would expect it to exhibit almost no observable deformations from the isolated molecule. We report results from the two refinements described earlier; the upper results are from the refinement which varied thermal parameters on the C atoms, and the lower results incorporated fixed neutron thermal parameters on all atoms. The difference between the two sets of experimental results is most striking, and the values obtaining by fixing thermal parameters at the neutron values are clearly superior and in excellent quantitative agreement with all of the components of the 6-31G** tensor. The diffraction estimate for $\langle r^2 \rangle$ of −337.9 (59) is in accord with the 6-31G** result of −342.3. This behavior is quite different to that observed for water, urea, imidazole, and cytosine, and it is tempting to ascribe it to the effect of hydrogen bonding in the latter cases. Finally for benzene we note that in spite of the quantitative agreement between the best diffraction estimates of second moments and corresponding ab initio results, diagonalization of the two tensors yields eigenvalues of (−134.2, −103.6, −100.1) from the multipole model and (−133.0, −104.9, −104.5) from ab initio theory, from which the quadrupole moments in Table V were obtained. Clearly the apparently small experimental errors reported for $\mu_{\alpha\beta}$ in Table VI can considerably compromise the reduction to quadrupole moment components.

We would have expected the results in Table VI for *p*-dicyanotetrafluorobenzene to echo those for benzene since this molecule also does not form hydrogen bonds. However, this is not the case; rather we see that both diffraction estimates (upper values from summation of pseudoatom multipoles, lower values from stockholder partitioning of the model electron density in the crystal) are essentially in agreement with each other (Hirshfeld[229] reported error estimates for only the upper set) and yield a lower estimate of μ_{xx} (along the C–N bonds) but a higher value of the other in-plane component, μ_{yy}. In contrast the out-of-plane component agrees well with the ab initio result, in accord with results for urea and benzene above. This concordance for the in-plane component is readily explained by the lack of any mechanism to transfer substantial amounts of charge out of the plane of these planar molecules; in contrast small amounts of charge transfer in the plane (as a consequence of intermolecular interactions) can readily alter the in-plane second moments.

VI. Summary and Generalizations

In this article we have attempted to draw together the results of electric dipole and quadrupole moment determinations from a very wide range of analyses of X-ray and neutron diffraction data, and critically assess them with an awareness of other experimental and theoretical results. We have discussed the strengths and weaknesses of the more commonly used experimental techniques for determining these properties and assessed the diffraction results in the light of this. In some detail we have discussed each of the results so far obtained for dipole and quadrupole moments using diffraction data and examined the use of second moments rather than quadrupole moments in the reporting of these properties. The great value of a study such as this is its scope and the way in which important trends and generalizations can be derived from the close examination of many studies and how we may readily arrive at conclusions which are not apparent from the results of one or two experiments. In this section we summarize the most important outcomes of this investigation and provide some, hopefully useful, generalizations regarding the extraction of electric moments from diffraction data.

(1) *The magnitude of the dipole moment is reliably determined and clearly demonstrates the effects of intermolecular interactions in the crystal.* Almost without exception this is observed to be the case, even with results derived from lower quality (e.g. room temperature, low resolution) data. Moreover, the results clearly seem to reflect the importance of intermolecular interactions in the crystal, particularly hydrogen bonding, as evidenced by significant enhancements over gas-phase or solution values in many instances. Typical errors in μ from diffraction data are between 2 and 4×10^{-30} C m (or approximately 1 Debye, much as predicted some time ago by Stewart[165]).

(2) *The direction of the dipole moment is reliably obtained.* Certainly the sense of the molecular dipole is always correct (except possibly where μ is small), and from the limited evidence available, the direction of the dipole moment vector is within 10° of independent experimental or theoretical estimates. Unfortunately the small number of comparisons available and the typical experimental error of ±10° in this direction precludes ascribing differences from isolated molecule results to the effects of intermolecular interaction.

(3) *The quadrupole moment can be reliably obtained.* This is particularly true for molecules which participate in only weak intermolecular interactions in the crystal.

(4) *Second moments are to be preferred over quadrupole moments.* The quadrupole moment tensor can be obtained from the second-moment tensor, but not vice versa; this alone suggests a preference for reporting second moments. However, as observed especially for hydrogen-bonded structures, any attempt to compare with other results can be hopelessly compromised if traceless quadrupole moment tensors are used. An important observation in this regard is that although the individual elements of the second-moment tensor may be obtained with a typical error of 3 to 10×10^{-40} C m^2 (approximately 5% to 10% for diagonal terms), this relative error is magnified considerably when applied to the quadrupole moment components.

(5) *Quadrupole and second moments seem to display the effects of intermolecular interactions.* This may be somewhat obvious, and much as expected, but the point here is that these effects appear to be significant and observable outcomes of the analysis of diffraction data. There is some evidence that the molecular electron cloud is not only polarized upon hydrogen bonding, but also undergoes a significant contraction in some directions.

(6) *Monopole (point charge) refinements are capable of yielding excellent estimates of dipole and quadrupole moments.* The success of the simple monopole refinement, whether it be the κ-refinement or Stewart's L-shell refinement, is clear. Even with data of modest quality it seems capable of providing a reliable estimate of the lower electric moments, and hence of the electrostatic potential. On reflection, this is perhaps not a surprising result, as although the monopole functions have been obtained by a fit to the electron density in the crystal (through the observable structure factors) they could equally well have been obtained by a fit to the electrostatic potential. This is because a fit to the electrostatic potential is formally equivalent to the use of a weighting function proportional to S^{-2} [i.e. $(\sin\theta/\lambda)^{-2}$] in the least-squares residual (eq 20). Stewart[242] has demonstrated the *exact* equivalence of multipole expansions obtained from fits weighted by any positive definite weight function in the limit of perfect data of infinite resolution, and it can be anticipated that similar considerations would apply to conventional X-ray data. Therefore we should *expect* that monopole refinements of the diffraction data would yield a set of point charges which are akin to those obtained by least-squares fitting to the electrostatic potential. This procedure is becoming increasingly popular for obtaining sets of point charges from ab initio wave functions[243,244] in order to estimate the electrostatic part of molecular interaction energies in molecular modeling studies, particularly where large numbers of molecules are involved (e.g. solute–solvent interactions, liquids, hydration of macromolecules). It is not inconceivable that diffraction experiments will be undertaken in the near future to determine sets of points charges for such purposes for molecules which are too large to be handled by theoretical techniques.

(7) *The better the diffraction data, the more reliable the result.* Again, this may seem self-evident, but it is repeatedly borne out by the studies discussed in this article. The best results (i.e. most accurate and precise) are usually obtained from extensive sets of low temperature X-ray data, usually in conjunction with neutron data collected at the same temperature. Collection of room-temperature data for any studies such as these would not seem to be worthwhile.

(8) *Estimates of experimental errors should always be reported.* The most compelling results discussed in this review have been accompanied by error estimates; without these it is virtually impossible to make a critical comparison with other measurements or assess a confidence interval in the results. However, it is worthwhile emphasizing that the errors quoted here have not all been derived in a consistent manner, and to our knowledge none include correlations between multipole populations (i.e. the complete inverse least-squares matrix). And it will always be true that because

of their means of derivation (eq 28) such errors are origin dependent and hence never definitive; it is always possible, however, to provide a *minimum* error.

(9) *Choice of thermal parameters seems to affect quadrupole and second-moment results.* Yet again, this is a sensible observation, as both local quadrupole deformations of the electron density and harmonic nuclear probability distribution functions have the same symmetry, but it has not been seriously considered in studies of electric moments to date. The results for benzene indicate that thermal parameters obtained from a separate neutron study, where they are totally unbiased by the electron distribution, are preferable to those obtained simultaneously in the X-ray analysis. This raises questions about results reported for imidazole and cytosine (among many others) where neutron position parameters were employed for all atoms, but neutral thermal parameters only for the hydrogen atoms. Further work exploring this aspect of the analysis would be profitable.

(10) *The best of these electron distributions should be used to further examine energies of intermolecular interactions in crystals.* A first step in this direction has been made by Spackman, Weber, and Craven,[164] but the reliability of diffraction estimates of dipole and quadrupole moments indicates that further work in this area is warranted, especially because the computations involved are rapid and quite straightforward compared to the actual multipole refinement procedure.

(11) *Many more model studies are required.* It is imperative to determine how reliably these lower electric moments can be obtained by either direct integration or multipole refinement strategies and whether there are any systematic errors resulting from the use of any of the strategies. There have been a very small number of such studies to date (those on formamide,[170] pyrazine,[235] urea,[115] and oxalic acid dihydrate,[241,245] although the latter two did not explore molecular moments obtained from the theoretical data) and the results obtained appear to be somewhat contradictory and not supported by the large body of experimental results. The ready availability of high quality ab initio wave functions for molecules, and more recently for molecular crystals,[246,247] opens the way for analyses of theoretical data on molecular crystals, both without and including the effects of intermolecular interactions.

Are we in a position now to recommend that X-ray (and neutron) data be collected for the express purpose of determining electric moments of molecules? Certainly not for the dipole moments, which can be obtained more readily by conventional means. At this stage the answer is also probably not for the quadrupole (or second) moment, but it is possible that such studies could be justified in the near future, once the method has been calibrated a little more with further careful experimental and model theoretical studies. This would seem to be especially true for molecules which form weak intermolecular interactions in the crystal; possibilities might include *s*-triazine and C_6F_6.

We doubt, however, that such studies would ever become commonplace. The wonderful advantage of the Bragg X-ray diffraction experiment is that it provides such a wealth of information on the electron distribution. Unlike other experiments which probe electric moments, the X-ray experiment is capable of yielding a three-dimensional parametric representation of the total electron distribution, and with increasing accuracy and precision all the time. This electron distribution has been most widely used in the past to explore chemical bonding, but the wealth of studies summarized in this article strongly suggests that molecular dipole and higher moments should be more commonly reported, even if only as a byproduct of a more conventional study of the electron density. And as we better understand the limitations of the method, there is a vast amount of information on intermolecular interactions which must be accessible in the future, either through the effects on observed electric moments or a computation of the energies involved.

Acknowledgments. By its very nature this work has relied heavily on the dedication and hard work of others. To all my colleagues engaged in the pursuit of charge densities from diffraction data I express my appreciation of those efforts. Some of this work was originally presented at the International Symposium on Accuracy in Structure Factor Measurement held in 1987 and further elaborated on for a presentation at the Gordon Research Conference on Electron Distributions and Chemical Bonding in 1989. I greatly appreciated the interaction with participants at those meetings, in particular Profs. Riccardo Destro and Dirk Feil who encouraged the writing of this article. The contributions made by Dr. Grant Moss, who participated in many of the very early studies of this type, deserve mention; his work did much to alert me to the possibilities. Finally, the perspective on other experimental determinations of electric moments is largely a result of the last five years of most enjoyable interaction with Prof. Geoff Ritchie. The responsibility for any errors or omissions, however, is solely mine.

VII. References

(1) Buckingham, A. D. *Adv. Chem. Phys.* **1967**, *12*, 107–142.
(2) Buckingham, A. D. *Quart. Rev.* **1959**, *13*, 183–214.
(3) Gray, C. G.; Gubbins, K. E. *Theory of Molecular Fluids. Volume 1: Fundamentals*; Clarendon Press: Oxford, 1984.
(4) Maitland, G. C.; Rigby, M.; Smith, E. B.; Wakeham, W. A. *Intermolecular Forces*; Oxford University Press: Oxford, 1981.
(5) Pertsin, A. J.; Kitaigorodsky, A. I. *The Atom-Atom Potential Method*; Springer-Verlag: Berlin, 1987.
(6) Hobza, P.; Zahradnik, R. *Intermolecular Complexes*; Elsevier: Amsterdam, 1988.
(7) Buckingham, A. D. In *Intermolecular Interactions: From Diatomics to Biopolymers*; Pullman, B., Ed.; John Wiley: New York, 1978; pp 1–67.
(8) Stone, A. J. In *Molecular Liquids—Dynamics and Interactions*; Barnes, A. J., Orville-Thomas, W. J., Yarwood, J., Eds.; D. Reidel: New York, 1984; pp 1–34.
(9) Hirschfelder, J. O.; Curtiss, C. F.; Bird, R. B. *Molecular Theory of Gases and Liquids*; Wiley: New York, 1954.
(10) Margenau, H.; Kestner, N. R. *Theory of Intermolecular Forces*; Pergamon Press: Oxford, 1971.
(11) Buckingham, A. D. In *Physical Chemistry. An Advanced Treatise*; Henderson, D., Ed.; Academic Press: New York, 1970; Vol. 4. (*Molecular Properties*), pp 349–386.
(12) Stewart, R. F. *J. Chem. Phys.* **1970**, *53*, 205–213.
(13) Kulakowska, I.; Geller, M.; Lesyng, B.; Wierzchowski, K. L. *Biochim. Biophys. Acta* **1974**, *361*, 119–130.
(14) McClellan, A. L. *Tables of Experimental Dipole Moments*; Rahara Enterprises: El Cerrito, 1989; Vol. 3.
(15) Applequist, J. *Chem. Phys.* **1984**, *85*, 279–290.
(16) Böttcher, C. J. F.; van Belle, O. C.; Bordewijk, P.; Rip, A. *Theory of Electric Polarization*, 2nd ed.; Elsevier: Amsterdam, 1973; Vol. 1.
(17) Stogryn, D. E.; Stogryn, A. P. *Mol. Phys.* **1966**, *11*, 371–393.
(18) McLean, A. D.; Yoshimine, M. *J. Chem. Phys.* **1967**, *47*, 3256–3262.
(19) Bogaard, M. P.; Buckingham, A. D.; Pierens, R. K.; White, A. H. *J. Chem. Soc., Faraday Trans. 1* **1978**, *74*, 3008–3015.

(20) Mulder, F.; van Hemert, M.; Wormer, P. E. S.; van der Avoird, A. *Theor. Chim. Acta* **1977**, *46*, 39–62.
(21) Mulder, F.; Thomas, G. F.; Meath, W. J. *Mol. Phys.* **1980**, *41*, 249–269.
(22) Visser, F.; Wormer, P. E. S.; Stam, P. *J. Chem. Phys.* **1983**, *79*, 4973–4984.
(23) Stone, A. J. *Chem. Phys. Lett.* **1981**, *83*, 233–239.
(24) Stone, A. J.; Tough, R. J. A. *Chem. Phys. Lett.* **1984**, *110*, 123–129.
(25) Stone, A. J.; Alderton, M. *Mol. Phys.* **1985**, *56*, 1047–1064.
(26) Stone, A. J.; Price, S. L. *J. Phys. Chem.* **1988**, *92*, 3325–3335.
(27) Price, S. L.; Stone, A. J.; Alderton, M. *Mol. Phys.* **1984**, *52*, 987–1001.
(28) Maslen, E. N.; Ridout, S. C.; Watson, K. J. *Acta Crystallogr., Sect. B* **1988**, *44*, 96–101.
(29) Maslen, E. N.; Watson, K. J.; Moore, F. H. *Acta Crystallogr., Sect. B* **1988**, *44*, 102–107.
(30) Bats, J. W.; Coppens, P.; Koetzle, T. F. *Acta Crystallogr., Sect. B* **1977**, *33*, 37–45.
(31) Coppens, P. In *MTP International Review of Science. Physical Chemistry Series 2*; Robertson, J. M., Ed.; Butterworths: London, 1975; Vol. 11 (*Chemical Crystallography*), p 21–56.
(32) Stevens, E. D.; Coppens, P.; Feld, R.; Lehmann, M. S. *Chem. Phys. Lett.* **1979**, *67*, 541–543.
(33) Stevens, E. D.; Coppens, P. *Acta Crystallogr., Sect. B* **1980**, *36*, 1864–1876.
(34) Hirshfeld, F. L. *Theor. Chim. Acta* **1977**, *44*, 129–138.
(35) Moss, G.; Feil, D. *Acta Crystallogr., Sect. A* **1981**, *37*, 414–421.
(36) Cohen, E. R.; Taylor, B. N. *J. Res. Natl. Bur. Stand.* **1987**, *92*, 85–95.
(37) McClellan, A. L. *Tables of Experimental Dipole Moments*; Rahara Enterprises: El Cerrito, 1974; Vol. 2.
(38) McClellan, A. L. *Tables of Experimental Dipole Moments*; Freeman: San Francisco, 1963.
(39) Madelung, O. *Landolt-Börnstein: Numerical Data and Functional Relationships in Science and Technology*; Springer-Verlag: Berlin, (*New Series, Group II: Atomic and Molecular Physics*); Vols. II/4 (1967), II/6 (1974), II/14a (1982), II/14b (1983).
(40) Lovas, F. J. *J. Phys. Chem. Ref. Data* **1978**, *7*, 1445–1750.
(41) Lovas, F. J.; Tiemann, E. *J. Phys. Chem. Ref. Data* **1974**, *3*, 609–769.
(42) Huber, K. P.; Herzberg, G. *Constants of Diatomic Molecules*; Van Nostrand-Reinhold: New York, 1979.
(43) Kirouac, S.; Bose, T. K. *J. Chem. Phys.* **1973**, *59*, 3043–3047.
(44) Sutter, H.; Cole, R. H. *J. Chem. Phys.* **1970**, *52*, 132–139.
(45) Böttcher, C. J. F.; Bordewijk, P. *Theory of Electric Polarization*, 2nd ed.; Elsevier: Amsterdam, 1978; Vol. 2.
(46) Smyth, C. P. In *Techniques of Chemistry*; Weisberger, A., Rossiter, B. W., Eds.; Wiley: New York, 1972; Vol. I.
(47) Buckingham, A. D. In *MTP International Review of Science, Physical Chemistry Series 1*; Ramsay, D. A., Ed.; Butterworths: London, 1972; Vol. 3; pp 73–117.
(48) Muenter, J. S. *J. Mol. Spectrosc.* **1975**, *55*, 490–491.
(49) Gordy, W. L.; Cook, R. L. *Microwave Molecular Spectra*; Wiley: New York, 1984.
(50) Flygare, W. H. *Chem. Rev.* **1974**, *74*, 653–687.
(51) Flygare, W. H.; Benson, R. C. *Mol. Phys.* **1971**, *20*, 225–250.
(52) Buckingham, A. D.; Dunmur, D. A. *Trans. Faraday Soc.* **1968**, *64*, 1776–1783.
(53) Graham, C.; Pierrus, J.; Raab, R. E. *Mol. Phys.* **1989**, *67*, 939–955.
(54) Buckingham, A. D.; Graham, C.; Williams, J. H. *Mol. Phys.* **1983**, *49*, 703–710.
(55) Vrbancich, J.; Ritchie, G. L. D. *J. Chem. Soc., Faraday Trans. 2* **1980**, *76*, 648–659.
(56) Craven, I. E.; Hesling, M. R.; Laver, D. R.; Lukins, P. B.; Ritchie, G. L. D.; Vrbancich, J. *J. Phys. Chem.* **1989**, *93*, 627–631.
(57) Dennis, G. R.; Ritchie, G. L. D. *J. Phys. Chem.* **1991**, *95*, 656–660.
(58) Flygare, W. H. *Molecular Structure and Dynamics*; Prentice-Hall: Englewood Cliffs, New Jersey, 1978.
(59) Sutter, D. H.; Flygare, W. H. *Top. Curr. Chem.* **1976**, *63*, 89–196.
(60) Albinus, L.; Spieckermann, J.; Sutter, D. H. *J. Mol. Spectrosc.* **1989**, *133*, 128–147.
(61) Dymanus, A. In *MTP International Review of Science, Physical Chemistry Series 2*; Buckingham, A. D., Ed.; Butterworths: London, 1975; Vol. 3, pp 127–204.
(62) Dyke, T. R.; Muenter, J. S. In *MTP International Review of Science, Physical Chemistry Series 2*; Buckingham, A. D., Ed.; Butterworths: London, 1975; Vol. 2, pp 27–92.
(63) Verhoeven, J.; Dymanus, A. *J. Chem. Phys.* **1970**, *52*, 3222–3233.
(64) Rosenblum, B.; Nethercott, A. H.; Townes, C. H. *Phys. Rev.* **1958**, *109*, 400–412.
(65) Frisch, M. J.; Head-Gordon, M.; Schlegel, H. B.; Raghavachari, K.; Binkley, J. S.; Gonzalez, C.; Defrees, D. J.; Fox, D. J.; Whiteside, R. A.; Seeger, R.; Melius, C. F.; Baker, J.; Martin, R. L.; Kahn, L. R.; Stewart, J. J. P.; Fluder, E. M.; Topiol, S.; Pople, J. A. *GAUSSIAN 88*, Gaussian Inc.: Pittsburgh, 1988.
(66) Schmidt, M. W.; Boatz, J. A.; Baldridge, K. K.; Koseki, S.; Gordon, M. S.; Elbert, S. T.; Lam, B. GAMESS. *QCPE Bull.* **1987**, *7*, 115.
(67) Amos, R. D.; Rice, J. E. CADPAC: The Cambridge Analytic Derivatives Package, issue 4.0, 1987.
(68) Davidson, E. R.; Feller, D. *Chem. Rev.* **1986**, *86*, 681–696.
(69) Feller, D.; Davidson, E. R. In *Reviews in Computational Chemistry*; Lipkowitz, K. B., Boyd, D. B., Eds.; VCH: New York, 1990; pp 1–43.
(70) Dykstra, C. E. *Ab initio calculation of the structures and properties of molecules*; Elsevier: Amsterdam, 1988.
(71) Dykstra, C. E.; Liu, S.-Y.; Malik, D. J. *Adv. Chem. Phys.* **1989**, *75*, 37–111.
(72) Dykstra, C. E.; Augspurger, J. D.; Kirtman, B.; Malik, D. J. In *Reviews in Computational Chemistry*; Lipkowitz, K. B., Boyd, D. B., Eds.; VCH: New York, 1990; pp 83–118.
(73) Hehre, W. J.; Radom, L.; Schleyer, P. v. R.; Pople, J. A. *Ab Initio Molecular Orbital Theory*; John Wiley & Sons: New York, 1986.
(74) Sadlej, A. J. *Collect. Czech. Chem. Commun.* **1988**, *53*, 1995–2016.
(75) Sadlej, A. J. *Theor. Chim. Acta* **1991**, *79*, 123–140.
(76) Wolinski, K.; Sadlej, A. J.; Karlstrom, G. *Mol. Phys.* **1991**, *72*, 425–432.
(77) Feller, D.; Boyle, C. M.; Davidson, E. R. *J. Chem. Phys.* **1987**, *86*, 3424–3440.
(78) Bishop, D. M. *Rev. Mod. Phys.* **1990**, *62*, 343–374.
(79) Hehre, W. J.; Ditchfield, R.; Pople, J. A. *J. Chem. Phys.* **1972**, *56*, 2257–2261.
(80) Dill, J. D.; Allen, L. C.; Topp, W. C.; Pople, J. A. *J. Am. Chem. Soc.* **1975**, *97*, 7220–7226.
(81) Francl, M. M.; Pietro, W. J.; Hehre, W. J.; Binkley, J. S.; Gordon, M. S.; DeFrees, D. J.; Pople, J. A. *J. Chem. Phys.* **1982**, *77*, 3654–3665.
(82) Hariharan, P. C.; Pople, J. A. *Theor. Chim. Acta* **1973**, *28*, 213–222.
(83) Stewart, R. F. In *Critical Evaluation of Chemical and Physical Structural Information*; Lide, D. R., Paul, M. A., Eds.; National Academy of Sciences: Washington, 1974; pp 540–561.
(84) Stewart, R. F. *God. Jugosl. Cent. Kristalogr.* **1982**, *17*, 1–24.
(85) Spackman, M. A.; Stewart, R. F. In *Methods and applications in crystallographic computing*; Hall, S. R., Ashida, T., Eds.; Clarendon Press: Oxford, 1984; pp 302–320.
(86) Stewart, R. F. In *The Application of Charge Density Research to Chemistry and Drug Design*; Jeffrey, G. A., Piniella, J. F., Eds.; Plenum Press: New York, 1991; pp 63–102.
(87) Coppens, P.; Stevens, E. D. *Adv. Quantum Chem.* **1977**, *10*, 1–35.
(88) Coppens, P.; Moss, G.; Hansen, N. K. In *Computing in Crystallography*; Diamond, R., Ramaseshan, S., Venkatesan, K., Eds.; Indian Academy of Sciences: Bangalore, 1980; pp 16.01–16.18.
(89) Coppens, P.; Stevens, E. D. In *Electron and Magnetization Densities in Molecules and Solids*; Becker, P., Ed.; Plenum: New York, 1980; pp 447–472.
(90) Coppens, P. In *Electron Distributions and the Chemical Bond*; Coppens, P., Hall, M. B., Eds.; Plenum: New York, 1982; pp 61–92.
(91) Coppens, P. *J. Phys. Chem.* **1989**, *93*, 7979–7984.
(92) Coppens, P.; Feil, D. In *The Application of Charge Density Research to Chemistry and Drug Design*; Jeffrey, G. A., Piniella, J. F., Eds.; Plenum Press: New York, 1991; pp 7–22.
(93) Hirshfeld, F. L. *J. Mol. Struct.* **1985**, *130*, 125–141.
(94) Hirshfeld, F. L. In *Accurate Molecular Structures. Their Determination and Importance*; Domenicano, A., Hargittai, I., Eds.; IUCr, Oxford University Press: Oxford, 1992; pp 237–269.
(95) Craven, B. M.; Stewart, R. F. *Trans. ACA* **1990**, *26*, 1–18.
(96) Craven, B. M. In *Crystallographic Computing 4. Techniques and New Technologies*; Isaacs, N. W., Taylor, M. R., Eds.; Oxford University Press: Oxford, 1988; pp 211–220.
(97) Stewart, R. F. *Isr. J. Chem.* **1977**, *16*, 137–143.
(98) Stewart, R. F.; Feil, D. *Acta Crystallogr., Sect. A* **1980**, *36*, 503–509.
(99) Rees, B. *Isr. J. Chem.* **1977**, *16*, 180–186.
(100) Lehmann, M. S. In *Electron and Magnetization Densities in Molecules and Solids*; Becker, P., Ed.; Plenum: New York, 1980; pp 287–322.
(101) Blessing, R. H.; Lecomte, C. In *The Application of Charge Density Research to Chemistry and Drug Design*; Jeffrey, G. A., Piniella, J. F., Eds.; Plenum Press: New York, 1991; pp 155–186.
(102) Fuess, H. In *The Application of Charge Density Research to Chemistry and Drug Design*; Jeffrey, G. A., Piniella, J. F., Eds.; Plenum Press: New York, 1991; pp 225–240.
(103) Seiler, P. In *Accurate Molecular Structures. Their Determination and Importance*; Domenicano, A., Hargittai, I., Eds.; IUCr, Oxford University Press: Oxford, 1992; pp 170–198.
(104) Stevens, E. D. *Mol. Phys.* **1979**, *37*, 27–45.
(105) Weber, H.-P.; Craven, B. M. *Acta Crystallogr., Sect. B* **1990**, *46*, 532–538.
(106) Eisenstein, M. *Acta Crystallogr., Sect. B* **1988**, *44*, 412–426.
(107) Bats, J. W.; Fuess, H.; Elerman, Y. *Acta Crystallogr., Sect. B* **1986**, *42*, 552–557.
(108) Elerman, Y.; Bats, J. W.; Fuess, H. *Acta Crystallogr., Sect. C* **1983**, *39*, 515–518.
(109) Delaplane, R. G.; Tellgren, R.; Olovsson, I. *Acta Crystallogr., Sect. C* **1984**, *40*, 1800–1803.
(110) Delaplane, R. G.; Tellgren, R.; Olovsson, I. *Acta Crystallogr., Sect. B* **1990**, *46*, 361–370.
(111) Pearlman, D. A.; Kim, S.-H. *J. Mol. Biol.* **1990**, *211*, 171–187.
(112) Corfield, P. W. R.; Shore, S. G. *J. Am. Chem. Soc.* **1973**, *95*, 1480–1487.
(113) Koritsanszky, T.; Buschmann, J.; Denner, L.; Luger, P.; Knochel, A.; Haarich, M.; Patz, M. *J. Am. Chem. Soc.* **1991**, *113*, 8388–8398.

(114) Stevens, E. D. *Acta Crystallogr., Sect. B* **1978**, *34*, 544–551.
(115) Swaminathan, S.; Craven, B. M.; Spackman, M. A.; Stewart, R. F. *Acta Crystallogr., Sect. B* **1984**, *40*, 398–404.
(116) Swaminathan, S.; Craven, B. M.; McMullan, R. K. *Acta Crystallogr., Sect. B* **1984**, *40*, 300–306.
(117) Weber, H.-P.; Craven, B. M. *Acta Crystallogr., Sect. B* **1987**, *43*, 202–209.
(118) van Nes, G. J. H.; van Bolhuis, F. *Acta Crystallogr., Sect. B* **1979**, *35*, 2580–2593.
(119) van Nes, G. J. H.; Vos, A. *Acta Crystallogr., Sect. B* **1979**, *35*, 2593–2601.
(120) Hirshfeld, F. L.; Hope, H. *Acta Crystallogr., Sect. B* **1980**, *36*, 406–415.
(121) Berkovitch-Yellin, Z.; Leiserowitz, L.; Nader, F. *Acta Crystallogr., Sect. B* **1977**, *33*, 3670–3677.
(122) Swaminathan, S.; Craven, B. M. *Acta Crystallogr., Sect. B* **1984**, *40*, 511–518.
(123) Weber, H.-P.; McMullan, R. K.; Swaminathan, S.; Craven, B. M. *Acta Crystallogr., Sect. B* **1984**, *40*, 506–511.
(124) Fabius, B.; Cohen-Addad, C.; Larsen, F. K.; Lehmann, M. S.; Becker, P. *J. Am. Chem. Soc.* **1989**, *111*, 5728–5732.
(125) He, X. M.; Swaminathan, S.; Craven, B. M.; McMullan, R. K. *Acta Crystallogr., Sect. B* **1988**, *44*, 271–281.
(126) Craven, B. M.; McMullan, R. K. *Acta Crystallogr., Sect. B* **1979**, *35*, 934–945.
(127) Coppens, P. *Science* **1967**, *158*, 1577–1579.
(128) McMullan, R. K.; Epstein, J.; Ruble, J. R.; Craven, B. M. *Acta Crystallogr., Sect. B* **1979**, *35*, 688–691.
(129) Epstein, J.; Ruble, J. R.; Craven, B. M. *Acta Crystallogr., Sect. B* **1982**, *38*, 140–149.
(130) Destro, R.; Bianchi, R.; Morosi, G. *J. Phys. Chem.* **1989**, *93*, 4447–4457.
(131) Swaminathan, S.; Craven, B. M.; McMullan, R. K. *Acta Crystallogr., Sect. B* **1985**, *41*, 113–122.
(132) de With, G.; Harkema, S.; Feil, D. *Acta Crystallogr., Sect. B* **1976**, *32*, 3178–3184.
(133) Stewart, R. F.; Jensen, L. H. *Acta Crystallogr.* **1967**, *23*, 1102–1105.
(134) Weber, H. P.; Craven, B. M.; McMullan, R. K. *Acta Crystallogr., Sect. B* **1980**, *36*, 645–649.
(135) Kvick, A.; Koetzle, T. F.; Stevens, E. D. *J. Chem. Phys.* **1979**, *71*, 173–179.
(136) Kvick, A.; Al-Karaghouli, A. R.; Koetzle, T. F. *Acta Crystallogr., Sect. B* **1977**, *33*, 3796–3801.
(137) Craven, B. M.; Weber, H.-P. *Acta Crystallogr., Sect. B* **1983**, *39*, 743–748.
(138) Weber, H.-P.; Craven, B. M.; McMullan, R. K. *Acta Crystallogr., Sect. B* **1983**, *39*, 360–366.
(139) Wang, Y.; Blessing, R. H.; Ross, F. K.; Coppens, P. *Acta Crystallogr., Sect. B* **1976**, *32*, 572–578.
(140) Coppens, P. *Acta Crystallogr., Sect. B* **1976**, *32*, 1777–1784.
(141) Klooster, W. T.; Swaminathan, S.; Nanni, R.; Craven, B. M. *Acta Crystallogr., Sect. B* **1992**, *48*, 217–227.
(142) McMullan, R. K.; Craven, B. M. *Acta Crystallogr., Sect. B* **1989**, *45*, 270–276.
(143) Baert, F.; Schweiss, P.; Heger, G.; More, M. *J. Mol. Struct.* **1988**, *178*, 29–48.
(144) Jeffrey, G. A.; Lehmann, C. W.; Ruble, J. R.; Yeon, Y. Unpublished results 1989.
(145) Jeffrey, G. A.; Ruble, J. R.; McMullan, R. K.; Pople, J. A. *Proc. R. Soc. London, A* **1987**, *414*, 47–57.
(146) McMullan, R. K.; Benci, P.; Craven, B. M. *Acta Crystallogr., Sect. B* **1980**, *36*, 1424–1430.
(147) Craven, B. M.; Benci, P. *Acta Crystallogr., Sect. B* **1981**, *37*, 1584–1591.
(148) Dunitz, J. D.; Schweizer, W. B.; Seiler, P. *Helv. Chim. Acta* **1983**, *66*, 123–133.
(149) Baert, F.; Coppens, P.; Stevens, E. D.; Devos, L. *Acta Crystallogr., Sect. A* **1982**, *38*, 143–151.
(150) Devos, L.; Baert, F.; Fouret, R.; Thomas, M. *Acta Crystallogr., Sect. B* **1980**, *36*, 1807–1811.
(151) Craven, B. M.; Fox, R. O., Jr.; Weber, H.-P. *Acta Crystallogr., Sect. B* **1982**, *38*, 1942–1952.
(152) McMullan, R. K.; Fox, R. O., Jr.; Craven, B. M. *Acta Crystallogr., Sect. B* **1978**, *34*, 3719–3722.
(153) Rees, B.; Coppens, P. *Acta Crystallogr., Sect. B* **1973**, *29*, 2516–2528.
(154) Klooster, W. T.; Ruble, J. R.; Craven, B. M.; McMullan, R. K. *Acta Crystallogr., Sect. B* **1991**, *47*, 376–383.
(155) Klooster, W. T.; Craven, B. M. *Acta Crystallogr., Sect. B* **1992**, submitted for publication.
(156) Debye, P. *Physik. Z.* **1930**, *31*, 419–428.
(157) Hirshfeld, F. L. *Isr. J. Chem.* **1977**, *16*, 226–229.
(158) Hirshfeld, F. L. *Acta Crystallogr., Sect. B* **1971**, *27*, 769–781.
(159) Hansen, N. K.; Coppens, P. *Acta Crystallogr., Sect. A* **1978**, *34*, 909–921.
(160) Craven, B. M.; Weber, H.-P.; He, X. *The POP Procedure: Computer Programs to Derive Electrostatic Properties from Bragg Reflections*; University of Pittsburgh: Pittsburgh, 1987.
(161) Stewart, R. F.; Spackman, M. A. *VALRAY Users Manual*; Chemistry Department, Carnegie-Mellon University: Pittsburgh, PA, 1983.
(162) Stewart, R. F. *J. Chem. Phys.* **1973**, *58*, 1668–1676.
(163) Lecomte, C. In *The Application of Charge Density Research to Chemistry and Drug Design*; Jeffrey, G. A., Piniella, J. F., Eds.; Plenum Press: New York, 1991; pp 121–154.
(164) Spackman, M. A.; Weber, H.-P.; Craven, B. M. *J. Am. Chem. Soc.* **1988**, *110*, 775–782.
(165) Stewart, R. F. *J. Chem. Phys.* **1972**, *57*, 1664–1668.
(166) Coppens, P.; Guru Row, T. N.; Leung, P.; Stevens, E. D.; Becker, P. J.; Yang, Y. W. *Acta Crystallogr., Sect. A* **1979**, *35*, 63–72.
(167) Coppens, P.; Hamilton, W. C. *Acta Crystallogr., Sect. B* **1968**, *24*, 925–929.
(168) Coppens, P.; Hansen, N. K. *Isr. J. Chem.* **1977**, *16*, 163–167.
(169) Moss, G. In *Electron Distributions and the Chemical Bond*; Coppens, P., Hall, M. B., Eds.; Plenum: New York, 1982; pp 383–411.
(170) Moss, G.; Coppens, P. *Chem. Phys. Lett.* **1980**, *75*, 298–302.
(171) Coppens, P.; Guru-Row, T. N. *Ann. N.Y. Acad. Sci.* **1978**, *313*, 244–255.
(172) Bats, J. W.; Fuess, H. *Acta Crystallogr., Sect. B* **1986**, *42*, 26–32.
(173) Dyke, T. R.; Muenter, J. S. *J. Chem. Phys.* **1973**, *59*, 3125–3127.
(174) Sears, P. G.; Fortune, W. H.; Blumenshine, R. L. *J. Chem. Eng. Data* **1966**, *11*, 406–409.
(175) Leavers, D. R.; Taylor, W. T. *J. Phys. Chem.* **1977**, *81*, 2257–2260.
(176) Schneider, W. C. *J. Am. Chem. Soc.* **1950**, *72*, 761–763.
(177) Kurland, R. J.; Wilson, E. B. *J. Chem. Phys.* **1957**, *27*, 585–590.
(178) Aroney, M. J.; Le Fevre, R. J. W.; Singh, A. N. *J. Chem. Soc.* **1965**, 3179–3184.
(179) Brown, R. D.; Godfrey, P. D.; Storey, J. *J. Mol. Spectrosc.* **1975**, *58*, 445–450.
(180) Kumler, W. D.; Fohlen, G. M. *J. Am. Chem. Soc.* **1942**, *64*, 1944–1948.
(181) Lefebvre, J. *Solid State Commun.* **1973**, *13*, 1873–1875.
(182) Berkovitch-Yellin, Z.; Leiserowitz, L. *J. Am. Chem. Soc.* **1980**, *102*, 7677–7690.
(183) Kojima, T.; Yano, E.; Nakagawa, K.; Tsunekawa, S. *J. Mol. Spectrosc.* **1987**, *122*, 408–416.
(184) Larsen, N. W.; Nygaard, L.; Pedersen, T.; Pedersen, C. T.; Davy, H. *J. Mol. Struct.* **1984**, *118*, 89–95.
(185) Christen, D.; Griffiths, J. H.; Sheridan, J. *Z. Naturforsch.* **1982**, *37a*, 1378–1385.
(186) Calderbank, K. E.; Calvert, R. L.; Lukins, P. B.; Ritchie, G. L. D. *Aust. J. Chem.* **1981**, *34*, 1835–1844.
(187) Khanarian, G.; Moore, W. J. *Aust. J. Chem.* **1980**, *33*, 1727–1741.
(188) Stewart, R. F. In *Electron and Magnetization Densities in Molecules and Solids*; Becker, P., Ed.; Plenum: New York, 1980; pp 405–425.
(189) Yanez, M.; Stewart, R. F. *Acta Crystallogr., Sect. A* **1978**, *34*, 648–651.
(190) Palmer, M. H.; Wheeler, J. R.; Kwiatkowski, J. S.; Lesyng, B. *J. Mol. Struct.* **1983**, *92*, 283–302.
(191) Sakellaridis, P. U.; Karageorgopolous, E. K. *Z. Naturforsch.* **1974**, *29a*, 1834–1837.
(192) Edward, J. T.; Farrell, P. G.; Lob, J. L. *J. Phys. Chem.* **1973**, *77*, 2192–2195.
(193) Pottel, R.; Adolph, D.; Kaatze, U. *Ber. Bunsen-Ges. Phys. Chem.* **1975**, *79*, 278–285.
(194) Katritzky, A. R.; Randall, E. W.; Sutton, L. E. *J. Chem. Soc.* **1957**, 1769–1775.
(195) Bergmann, E. D.; Weiler-Feilchenfeld, H.; Neiman, Z. *J. Chem. Soc.* **1970**, *B*, 1334–1336.
(196) Treiner, C.; Skinner, J. F.; Fuoss, R. M. *J. Phys. Chem.* **1964**, *68*, 3406–3409.
(197) Soundararajan, S. *Trans. Faraday Soc.* **1958**, *54*, 1147–1150.
(198) Lumbroso, H.; Segard, C.; Roques, B. *J. Organometal. Chem.* **1973**, *61*, 249–260.
(199) Tyler, J. K.; Sheridan, J.; Costain, C. C. *J. Mol. Spectrosc.* **1972**, *43*, 248–261.
(200) Lefebvre, J. *Phys. Stat. Sol. (B)* **1972**, *49*, 673–684.
(201) Ruble, J. R.; Wang, A. C.; Craven, B. M. *J. Mol. Struct.* **1979**, *51*, 229–237.
(202) Cohen-Addad, C.; Lehmann, M. S.; Becker, P.; Davy, H. *Acta Crystallogr., Sect. B* **1988**, *44*, 522–527.
(203) Destro, R.; Marsh, R. E.; Bianchi, R. *J. Phys. Chem.* **1988**, *92*, 966–973.
(204) Hall, W. R. *J. Med. Chem.* **1977**, *20*, 275–279.
(205) Berthier, G.; Defranceschi, M.; Lazzeretti, P.; Tsoucaris, G.; Zanasi, R. *J. Mol. Struct.* **1992**, *254*, 205–218.
(206) Kyogoku, Y.; Lord, R. C.; Rich, A. *J. Am. Chem. Soc.* **1967**, *89*, 496–504.
(207) Varma, C. A. G. O.; Groenen, E. J. J. *Recl. Trav. Chim. Pays-Bas* **1972**, *91*, 296–316.
(208) Kurki-Suonio, K. *Isr. J. Chem.* **1977**, *16*, 132–136.
(209) Legon, A. C.; Millen, D. J. *Chem. Rev.* **1986**, *86*, 635–657.
(210) Hermansson, K.; Lunell, S. *Chem. Phys. Lett.* **1981**, *80*, 64–68.
(211) Lunell, S. *J. Chem. Phys.* **1984**, *80*, 6185–6193.
(212) Cummins, P. L.; Bacskay, G. B.; Hush, N. S. *Mol. Phys.* **1987**, *61*, 795–811.

(213) Cummins, P. L.; Bacskay, G. B.; Hush, N. S. *Mol. Phys.* **1987**, *62*, 193–213.

(214) Barnes, P.; Finney, J. L.; Nicholas, J. D.; Quinn, J. E. *Nature* **1979**, *282*, 459–464.

(215) Goodfellow, J. M.; Finney, J. L.; Barnes, P. *Proc. R. Soc. London, B* **1982**, *214*, 213–228.

(216) Buckingham, A. D.; Fowler, P. W.; Stone, A. J. *Int. Rev. Phys. Chem.* **1986**, *5*, 107–114.

(217) Fowler, P. W.; Stone, A. J. *J. Phys. Chem.* **1987**, *91*, 509–511.

(218) Sanchez de Meras, A. M.; Jensen, H. J. A.; Jorgensen, P.; Olsen, J. *Chem. Phys. Lett.* **1991**, *186*, 379–385.

(219) Emrich, R. J.; Steele, W. *Mol. Phys.* **1980**, *40*, 469–475.

(220) Tigelaar, H. L.; Flygare, W. H. *J. Am. Chem. Soc.* **1972**, *94*, 343–346.

(221) Coonan, M. H.; Ritchie, G. L. D. *Chem. Phys. Lett.* **1992**, submitted for publication.

(222) Kukolich, S. G.; Aldrich, P. D.; Read, W. G.; Campbell, E. J. *J. Chem. Phys.* **1983**, *79*, 1105–1110.

(223) Dagg, I. R.; Read, L. A. A.; Smith, W. *Can. J. Phys.* **1982**, *60*, 1431–1441.

(224) Price, P. F.; Maslen, E. N.; Delaney, W. T. *Acta Crystallogr., Sect. A* **1978**, *34*, 194–203.

(225) Dennis, G. R. Ph.D. Thesis, University of Sydney, 1986.

(226) Stolze, M.; Sutter, D. H. *Z. Naturforsch.* **1987**, *42a*, 49–56.

(227) Spackman, M. A. Unpublished results, 1991,

(228) Battaglia, M. R.; Buckingham, A. D.; Williams, J. H. *Chem. Phys. Lett.* **1981**, *78*, 421–423.

(229) Hirshfeld, F. L. *Acta Crystallogr., Sect. B* **1984**, *40*, 484–492.

(230) Stevens reported a radial exponent of 4.0 Å^{-1} for single exponential radial functions in all refinements, but this is an error (Stevens, E. D. Personal communication, 1992) and should be 4.0 au^{-1}; we have used 4.0 au^{-1} in our calculations.

(231) Gordy, W.; Smith, W. V.; Trambarulo, R. F. *Microwave Spectroscopy*; Wiley: New York, 1953.

(232) Lindh, R.; Liu, B. *J. Chem. Phys.* **1991**, *94*, 4356–4368.

(233) Mason, R.; Rae, A. I. M. *Proc. R. Soc. London A* **1968**, *304*, 501–512.

(234) Walker, I. C.; Palmer, M. H. *Chem. Phys.* **1991**, *152*, 169–187.

(235) Feil, D.; Moss, G. *Acta Crystallogr., Sect. A* **1983**, *39*, 14–21.

(236) Almlof, J.; Roos, B.; Wahlgren, U.; Johansen, H. *J. Electron Spectrosc. Rel. Phenom.* **1973**, *2*, 51–74.

(237) Delley, B. *Chem. Phys.* **1986**, *110*, 329–338.

(238) Clementi, E. *IBM J. Res. Develop.* **1965**, *9*, Supplement.

(239) Clementi, E.; Roetti, C. *At. Data Nucl. Data Tables* **1974**, *14*, 177–478.

(240) Boyd, R. J. *Can. J. Phys.* **1977**, *55*, 452–455.

(241) Krijn, M. P. C. M.; Feil, D. *J. Chem. Phys.* **1988**, *89*, 4199–4208.

(242) Stewart, R. F. *Isr. J. Chem.* **1977**, *16*, 124–131.

(243) Cox, S. R.; Williams, D. E. *J. Comput. Chem.* **1981**, *2*, 304–323.

(244) Chirlian, L. E.; Francl, M. M. *J. Comput. Chem.* **1987**, *8*, 894–905.

(245) Krijn, M. P. C. M.; Graafsma, H.; Feil, D. *Acta Crystallogr., Sect. B* **1988**, *44*, 609–616.

(246) Dovesi, R.; Pisani, C.; Roetti, C.; Causa, M.; Saunders, V. R. CRYSTAL 88, Program # 577. *Quantum Chemistry Program Exchange*; Indiana University: Bloomington, IN, 1988.

(247) Dovesi, R.; Causa, M.; Orlando, R.; Roetti, C.; Saunders, V. R. *J. Chem. Phys.* **1990**, *92*, 7402–7411.